OCEAN DRILLING PROGRAM

LEG 166 PRELIMINARY REPORT

THE BAHAMAS TRANSECT

Dr. Gregor Eberli
Co-Chief Scientist, Leg 166
Rosentiel School for Marine and
Atmospheric Sciences
University of Miami
4600 Rickenbacker Causeway
Miami, Florida 33149
U.S.A.

Dr. Peter Swart
Co-Chief Scientist, Leg 166
Rosentiel School for Marine and
Atmospheric Sciences
University of Miami
4600 Rickenbacker Causeway
Miami, Florida 33149
U.S.A.

Dr. Mitchell Malone
Staff Scientist, Leg 166
Ocean Drilling Program
Texas A&M University Research Park
1000 Discovery Drive
College Station, Texas 77845-9547
U.S.A.

____
Paul J. Fox
Director
Science Operations
ODP/TAMU

____
Jack Baldauf
Manager
Science Operations
ODP/TAMU

____
Timothy J.G. Francis
Deputy Director
Science Operations
ODP/TAMU

May 1996

Preliminary Report No. 66

First Printing 1996

Distribution

Electronic copies of this report can be found on the ODP Publications Home Page on the World Wide Web at http://www-odp.tamu.edu/publications.

D I S C L A I M E R

This publication was prepared by the Ocean Drilling Program, Texas A&M University, as an account of work performed under the international Ocean Drilling Program, which is managed by Joint Oceanographic Institutions, Inc., under contract with the National Science Foundation. Funding for the program is provided by the following agencies:

Canada/Australia Consortium for the Ocean Drilling Program
Deutsche Forschungsgemeinschaft (Federal Republic of Germany)
Institut Français de Recherche pour l'Exploitation de la Mer (France)
Ocean Research Institute of the University of Tokyo (Japan)
National Science Foundation (United States)
Natural Environment Research Council (United Kingdom)
European Science Foundation Consortium for the Ocean Drilling Program (Belgium, Denmark, Finland, Iceland, Italy, The Netherlands, Norway, Spain, Sweden, Switzerland, and Turkey)

SCIENTIFIC REPORT

The following scientists were aboard the *JOIDES Resolution* for Leg 166 of the Ocean Drilling Program:

Gregor Eberli, Co-Chief Scientist, (RSMAS-MGG, University of Miami, 4600 Rickenbacker Cswy., Miami, FL 33149, U.S.A.; E-mail: geberli@rsmas.miami.edu)

Peter Swart, Co-Chief Scientist, (RSMAS-MGG, University of Miami, 4600 Rickenbacker Cswy., Miami, FL 33149, U.S.A.; E-mail: pswart@rsmas.miami.edu)

Mitchell Malone, Staff Scientist, (Ocean Drilling Program, 1000 Discovery Drive, Texas A&M University, College Station, TX, U.S.A.; E-mail: mitchell_malone@odp.tamu.edu)

Flavio S. Anselmetti, Physical Properties Specialist, (RSMAS , University of Miami, 4600 Rickenbacker Cswy., Miami, FL 33149, U.S.A., E-mail: anselmetti@rcf.rsmas.miami.edu)

Kohsaku Arai, Sedimentologist, (Geological Survey of Japan, 1-1-3 Higashi, Tsukuba, Ibarki, 305 Japan, E-mail: kohsaku@gsj.go.jp)

Karin H. Bernet, Sedimentologist, (University of Miami, RSMAS-MGG, 4600 Rickenbacker Cswy., Miami, FL 33149, U.S.A., E-mail: bernet@rsmas.miami.edu)

Christian Betzler, Sedimentologist, (Geologisch-Paläontologisches Institut, Johann Wolfgang Goethe-Universität, Frankfurt-am-Main, Senskenberganlage 32-34, Postfach 11 19 32, D-60325 Frankfurt-am-Main, Federal Republic of Germany, E-mail: betzler@em.uni-frankfurt.d400.de)

Beth A. Christensen, Stratigraphic Correlator, (Dept. of Geological Sciences, University of South Carolina, Columbia, SC 29208, U.S.A., E-mail: bac@paleo.geol.scarolina.edu)

Eric H. De Carlo, Inorganic Geochemist, (Dept. of Oceanography/SOEST, University of Hawaii, 1000 Pope Road, Honolulu, HI 96822, E-mail: edecarlo@soest.hawaii.edu)

Pascale Déjardin, Sedimentologist, (Centre de Sédimentologie et de Géochimie de la Surface, CNRS, 1 rue Blessig, Strasbourg cedex 67084, France, E-mail: dejardin@illite.u-strasg.fr)

Laurent Emmanuel, Sedimentologist (University of Bourgogne, Centre des Sciences de la Terre, 6. Blvd Gabriel, F-21000 Dijon, France, E-mail: lemmanue@satie.u-bourgogne.fr.edu)

Tracy Frank, Sedimentologist, (Dept. of Geological Sciences, University of Michigan, 2534 C.C. Little Bldg., Ann Arbor, MI, U.S.A.; E-mail: tdfrank@umich.edu)

Geoffrey A. Haddad, Sedimentologist, (Dept. of Geology & Geophysics, Rice University, MS 126, 6100 South Main Street, Houston, TX 77005-1892, U.S.A., E-mail: ghaddad@geophysics.rice.edu)

Alexandra R. Isern, Physical Properties Specialist, (Dept. of Geology & Geophysics, University of Sydney, Sydney, NSW 2006, Australia, E-mail: aisern@es.su.oz.au)

Miriam E. Katz, Paleontologist (benthic foraminifers), (Lamont-Doherty Earth Observatory, Columbia University, Palisades, NY 10964, U.S.A., E-mail: mkatz@ldeo.columbia.edu)

Jeroen A.M. Kenter, Physical Properties Specialist, (Dept. of Earth Sciences, Vrije Universiteit, De Boelelaan 1085, 1081 HV Amsterdam, The Netherlands, E-mail: kenj@geo.vu.nl)

Philip A. Kramer, Inorganic Geochemist, (Institute of Marine and Coastal Studies, Nova University, 800 N. Ocean Dr., Dania, FL 33004, U.S.A.)

Dick Kroon, Paleontologist (planktonic foraminifers), (Dept. of Geology & Geophysics, Grant Institute, University of Edinburgh, King’s Bldgs., West Mains Road, EH9 3JW Edinburgh, Scotland, United Kingdom, E-mail: dkroon@glg.ed.ac.uk)

Judith A. McKenzie, JOIDES Logging Scientist, (Geological Institute, ETH-Zentrum, 8092 Zürich, Switzerland, E-mail: sediment@erdw.ethz.ch)

Donald F. McNeill, Paleomagnetist (RSMAS, University of Miami, 4600 Rickenbacker Cswy., Miami, FL 33149, U.S.A., E-mail: dmcneill@rsmas.miami.edu)

Paul Montgomery, Paleomagnetist, (School of Environmental Science, University of East

Anglia, Norwich NR4 7TJ, United Kingdom)
Seiichi Nagihara, Physical Properties Specialist, (Dept. of Geosciences, University of Houston, Houston, TX 77204-5503, U.S.A., E-mail: nagihara@uh.edu)
Carlos Pirmez, LDEO Logger, (Lamont-Doherty Earth Observatory, Columbia University, Borehole Research Group, Palisades, NY 10964, U.S.A., E-mail: pirmez@ldeo.columbia.edu)
John Reijmer, Sedimentologist, (GEOMAR, Christian-Albrechts-Universität zu Kiel, Wischhofstrasse 1-3, Gebäude 4, D-24148 Kiel, Federal Republic of Germany, E-mail: jreijmer@geomar.de)
Tokiyuki Sato, Paleontologist (nannofossils), (Institute of Applied Sciences, Mining College, Akita University, Tegata-Gakuencho 1-1, Akita 010, Japan, E-mail: toki@quartet.ipc.akita-u.ac.jp)
Niels Schovsbo, Organic Geochemist, (University of Copenhagen, Geological Museum, Oster Voldgade 5-7, DK1350K, Copenhagen, Denmark; E-mail: Niels@savik.geomus.ku.dk)
Trevor Williams, LDEO Logger Trainee, (Leichester University Borehole Research, Leichester University, Dept. of Geology, Leicester, LEI 7RH, United Kingdom, E-mail: tw7@le.ac.uk)
James D. Wright, Paleontologist (planktonic foraminifers), (Dept. of Geological Sciences, Sawyer Environmental Research Center, University of Maine, Orono, ME 04469, U.S.A. E-mail: jwright@maine.maine.edu)

ABSTRACT

Ocean Drilling Program Leg 166 drilled a total of 17 holes at seven sites (Sites 1003 through 1009) on the western flank of the Great Bahama Bank, recovering almost 3 km of core ranging in age from late Oligocene to Holocene. Leg 166 was designed to address two important geologic themes: (1) causes and effects of eustatic sea-level fluctuations and (2) fluid-flow processes in the margins of isolated platforms. To address fundamental questions regarding sea level fluctuations, five sites in the Straits of Florida were drilled (Sites 1003-1007), completing a transect through prograding carbonate sequences formed in response to sea-level fluctuations along the western margin of the Great Bahama Bank. Two boreholes (Clino and Unda) drilled previously on the western Great Bahama Bank as part of the Bahamas Drilling Project represent the shallow-water sites of the transect. The primary goal of the transect was to document the record of the Neogene–Holocene sea-level changes by determining the ages of the major unconformities in the sedimentary record and comparing the timing of these unconformities with ages predicted from the oxygen isotopic record of glacio-eustasy. Core borings from the complete transect document the facies variations associated with oscillations of sea level, and, therefore, the sedimentary response of the carbonate environment to sea-level changes. The correlation between the two independent records of sea-level changes, sequence stratigraphy and oxygen isotope proxy, has the potential to evaluate rate and amplitude of eustatic vs. relative sea-level changes and to establish a causal link between glacio-eustasy and the stratigraphic pattern.

With the sedimentary sequence recovered in advanced hydraulic piston coring, extended core barrel, and rotary core barrel drilling and the abundance of biostratigraphic markers, it was possible to define the ages of the Neogene sequence boundaries and to test their consistency with ages determined in the boreholes previously drilled on the platform. This yielded an excellent correlation between sites, documenting the age consistency of the sequence boundaries and chronostratigraphic significance of the seismic reflections. By reaching the Oligocene at Site 1007, a complete record for the sequence stratigraphic architecture is available for the entire Neogene. At all five transect sites (Sites 1003, 1004, 1005, 1006, and 1007), alternating high (up to 15 to 20 cm/k.y.) and low sedimentation rates (<2 cm/k.y.) reflect a long-term pattern of (1) bank flooding (0.5-2 m.y.), (2) concomitant shedding to the slope and periods of exposed banks, (3) a shutdown of shallow-water carbonate production, and (4) largely pelagic sedimentation. The pulses of bank-derived material coincide with the prograding pulses seen in the seismic data as sequences, which with their geometries indicate base-level lowerings as a result of sea-level falls.

Within these long-term changes, high-frequency sea-level changes are recorded in decimeter-scale depositional cycles. The ages of 17 seismic sequence boundaries (SSB) were determined. On the slope sites, several of these sequence boundaries coincide with biostratigraphically detected hiatuses indicating erosion. In some cases, slightly older ages of the SSB, when compared to the more distal sites on the slope, also suggest erosional downcutting. Therefore, to determine the ages of the sea-level changes, the ages of the SSBs were taken at the conformable portion of the sequences. They yielded the following preliminary ages: 0.1, 0.6, 1.7, 3.1, 3.6, 5.6, 8.7, 9.4, 10.5, 12.1, 12.5, 15.1, 16.0, 18.2, 19.4, 23.2, and 23.7 Ma. A comparison of seismic sequences with the global sea-level curve indicates that nearly all major (third-order) sea-level changes are recorded along the Bahamas Transect. This cyclic sedimentation is best developed in the Pleistocene and Miocene. The Pleistocene cycles display the characteristics of well-documented periplatform aragonite cycles where an increase in aragonite content coincides with sea-level highstands. The Miocene cycles display a decimeter-thick alternation of light-colored, bioturbated, well-cemented biowackestones and less cemented, darker biowackestones with compacted burrows. The Miocene alternations are interpreted to reflect changes in the rate of neritic input (metastable aragonite and high-Mg calcite). Thus, the well-cemented wackestones represent higher neritic potential and have a greater diagenetic input than the less cemented intervals with less neritic input. Facies and diagenesis act in concert to produce petrophysical differences within the sedimentary section. Thus, log data closely image the sedimentary and stratigraphic record, and the sequence boundaries can be clearly identified on these data. Consequently, the logging data may also be used to fill in gaps in core recovery.

The second objective of Leg 166 was to investigate the possible fluid flow within carbonate platforms. To achieve this objective, the sites of the transect were complemented by three additional shallow holes on the upper slope (Sites 1004, 1008, and 1009). The composition of the interstitial fluids retained in the sediment are used to assess rate and flow mechanisms through the bank.

In the upper 20-40 m of all sites, pore-water chemistry profiles display near-normal seawater concentrations of all constituents. The zone is thickest and most pronounced in the proximal, upper slope sites (Sites 1003, 1004, and 1005). This zone probably experiences pervasive flushing of seawater that prevents diffusional gradients from developing between the overlying seawater and the underlying, more saline fluid. Below the flushed zone, diffusive processes dominate the gradients of conservative elements, whereas non-conservative constituents show changes that are locally controlled by reactions such as organic matter remineralization and the recrystallization of carbonate minerals. These reactions are a result of the high in situ abundance of organic material trapped within these marginal sediments during rapid Pliocene-Pleistocene platform shedding events. The organic matter provides the fuel that drives the early carbonate alteration reactions in these shallow sediments. Superimposed on these downhole trends below the flushed zone, changes in gradients (e.g., localized increases in SO_4 and Cl^-) at similar depths provide strong evidence that flow is at least partially horizontal and related to stratigraphic boundaries. The deep interstitial waters show concentrations of Cl^- and other minor elements that are elevated relative to seawater (nearly twice that of normal seawater at Site 1003). The source of this high Cl^- is at present not known, but it could result from upward migration of a high salinity brine from an evaporitic deposit deeper in the Straits of Florida or beneath the Great Bahama Bank.

INTRODUCTION

Scientific drilling during Ocean Drilling Program (ODP) Leg 166, the Bahamas Transect, addressed two important geologic themes: (1) causes and effects of eustatic sea-level fluctuations, and (2) fluid-flow processes in continental margins. These themes were identified as first-order priorities by several planning groups of ODP (COSOD II, 1988; JOI/USSAC Workshop El Paso [Watkins and Mountain, 1990]; JOI/USSAC Workshop Arrowhead [Kastner and Brass, 1990]; and the Long Range Planning Documents, [JOI, Inc., 1990, 1996]). Specific approaches and drilling strategies were recommended by the ODP planning structure to gather the data necessary to answer questions pertaining to these themes. Based on this mandate, Leg 166 was designed as an integrated investigation of the designated themes within the context of a carbonate platform setting.

Leg 166 is the second transect (Leg 150 on the siliciclastic New Jersey margin was the first) in the ODP effort to examine the record of sea-level changes within the paradigm of sequence stratigraphy following the criteria established by the aforementioned planning groups. During Leg 166, the *JOIDES Resolution* drilled a transect of five sites (Sites 1003, 1004, 1005, 1006, and 1007) on the western flank of the Great Bahama Bank (GBB) (Figs. 1, 2). Sites 1008 and 1009, drilled further south on the western margin, were dedicated primarily to addressing fluid-flow objectives.

ODP Leg 166 was devoted to obtaining a transect of cores to ascertain the timing and amplitude of Neogene sea-level changes. The GBB is an ideal location to assess sea-level changes because it combines three independent ways of measuring sea-level changes: (1) it is a flat-topped platform on a passive continental margin and because it is level, cores drilled into it should record sea-level variations with accuracy, (2) the prograding sequences on its margin should record sea-level changes in their stratigraphic pattern, and (3) the correlative deep-water deposits encode the $\delta^{18}O$ proxy of sea-level changes in their foraminiferal assemblages. Correlation of the glacio-eustatic oxygen isotopic record with the sequence stratigraphic pattern of sea-level change can potentially document a causal link between glacio-eustasy and the stratal pattern. This correlation should also provide insights into how high-frequency sea-level fluctuations are recorded in these sediments and how the stacking of these high-frequency cycles combines to produce the lower-order seismic sequences.
There is increasing evidence that there is active fluid movement deep within carbonate platforms, as demonstrated by the results from ODP Leg 133 on the Queensland Plateau,

Australia (Elderfield, et al., 1993), ODP Leg 143 in the Pacific (1993; Paull et al.,1995), and from the Bahamas Drilling Project (Swart et al., in press a, in press b). Evidence for fluid flow can be observed in temperature and geochemical profiles. Temperature measurements in the sediments can detect nondiffusive geothermal gradients that indicate water movement either into or out of the formation (e.g., Davies, McKenzie, Palmer-Julson, et al., 1991). In addition, geochemical interstitial water measurements can show the influence of waters other than those indigenous to the formation. In a manner analogous to the temperature profiles, a uniform profile with depth could indicate fluid movement into the formation. Conversely, a concave upwards profile could imply fluids moving out of the formation. Lateral fluid movement may be indicated by erratic changes in the nature of the geochemical or temperature profiles.

The sea-level-related objectives of ODP Leg 166 were to:

1. determine the timing of the sequence boundaries and relative sea-level fluctuations. The ages of these sequences will contribute to the database that is necessary eventually to evaluate the global synchrony of sea-level fluctuations in the Neogene;

2. determine the stratigraphic response of carbonates to sea-level changes by analyzing the facies of the recovered depositional sequences. A special emphasis was placed on documenting the amount and nature of lowstand deposits in carbonates and on the hierarchical stacking of high-frequency cycles into seismic sequences;

3. retrieve low-latitude isotope signals of the Icehouse World in the Neogene and Quaternary and compare it with the stratigraphic record to evaluate whether there is a causal link between eustasy and sequence stratigraphic pattern; and

4. estimate the magnitudes and rates of sea-level changes using ages and recovered facies for a precise subsidence analysis.

To accomplish the fluid-flow objectives, drilling was designed to:

1. assess the possibility that there is fluid flow into and out of the platform along the margins, and

2. test the proposed mechanisms of fluid flow.

To address these topics, seven sites were drilled on the western flank of GBB (Figs. 1, 2).

Site 1003 (proposed Site BT-2) is one of five sites along a transect connecting the shallow bank with the deeper water areas. Site 1003 is located on the middle slope of the prograding western margin of Great Bahama Bank, approximately 4 km from the platform edge and 12.6 km from the borehole Clino, which was drilled on the banktop from a self-propelled jack-up barge. The primary objectives of Site 1003 were to penetrate to the base of the Neogene to evaluate facies of lowstand vs. highstand deposits and to determine the respective amount of redeposited strata in both systems tracts. Additional objectives were (1) to refine the ages of the sequence boundaries, (2) to determine the nature of a prominent unconformity on top of a low-amplitude to transparent seismic zone at 0.75 s two-way traveltime (TWT) that is interpreted to be the top of the early Pliocene, (3) to produce a high-resolution isotope stratigraphy of the Neogene to Holocene, and (4) to evaluate fluid flow in the middle of the lower slope.

Site 1004 (proposed Site F-3) is located between Sites 1003 and 1005 on the same dip line. The primary objective of Site 1004 was to obtain heat-flow and interstitial water geochemistry measurements to be used in conjunction with data obtained from Sites 1003, 1005, 1006, and 1007 to ascertain possible fluid flow and diagenetic reactions in the carbonate margin. In addition, this site serves as a location for the study of high-resolution sea-level changes during the Pleistocene, adding information to the comprehensive sea-level objectives of Leg 166.

Site 1005 (proposed Site BT-1A/F-1) is the most proximal site of five sites along the Bahamas Transect from the western margin of GBB into the Straits of Florida. Operational safety considerations required relocating Site 1005 to deeper water than the originally proposed Prospectus location (BT-1/F-1). Site 1005 is located in 352 m water depth, approximately 1150 m from the modern platform edge on the upper slope, 30 shot points SW of the crossing of seismic lines 106 and 107. It is positioned on the thickest part of the prograding Neogene sequences seen on the seismic line. The target depth of 700 m was designed to penetrate seven seismic sequences. The sea-level objectives of Site 1005 were (1) to date the sequence boundaries precisely; (2) to determine the facies within the different systems tracts, especially the nature of the onlapping units that were interpreted as lowstand deposits; and (3) to retrieve a high-resolution record of climate and sea-level fluctuations for the Quaternary and late Pliocene. This site served also as the proximal site for the fluid-flow transect.

Site 1006, (proposed Site BT-5), is located in 650 m of water approximately 30 km from the western platform edge of Great Bahama Bank. It is the most distal of the five transect sites positioned at the crossing of seismic lines 105 and 106. Drilling at Site 1006 was designed to core and log a thick sequence of drift deposits, which are thought to extend through the Neogene with relatively few hiatuses. There were two principal objectives at this site. First, the sediments at Site 1006 were believed to have a greater pelagic component than the proximal sites (Sites 1003, 1004, 1005, and 1007) of the transect, so they should be well suited for dating and establishing an oxygen and strontium isotope stratigraphy for the Neogene, and thereby provide an independent indicator of sea level. These datums could be traced on the seismic reflections to the distal lobes of the prograding margins in the proximal sites. This approach will help date the proximal sites where the chronostratigraphy is occasionally unclear because of poor recovery, diagenesis, and/or dilution by neritic sediments. Second, changes in the sediment composition were postulated to vary in conjunction with variations in the strength of the Florida Current. These variations would correlate with changes in sea level, as recorded by the prograding and regressive sequences at platform sites and the oxygen isotopic signature of the foraminifers.

Site 1007 (proposed Site BT-3), at the crossing of seismic lines 106 and 102B, was located on the toe of the western Great Bahama Bank slope at a water depth of 647 m. The target depth was the base of the Neogene which was estimated to be at approximately 1230 mbsf. The site was positioned to penetrate the thin basinal portions of 16 prograding sequences and, in the upper part, a thick onlapping wedge that could be either a drift deposit or an accumulation of mass-gravity flows. To the west, the distal portions of the prograding clinoforms interfinger with the drift deposits of Site 1006. Site 1007, therefore, was the link between this basinal site and the proximal slope sites to the east. In addition, a higher content of microfossils with good preservation was expected than in the more proximal Sites 1005, 1004, and 1003. Therefore, the main sea-level objectives of this site were (1) to precisely date the sequence boundaries, (2) to determine the facies in the distal portions of carbonate sequences, and (3) to assemble a data set suitable to compare the sedimentary record with the oxygen isotope record of the Neogene to Holocene sea-level fluctuations. Site 1007 was also a intermediate site for the fluid-flow studies. Interstitial water chemistry and in situ temperature measurements at this site should provide information about the fluid movement in the lower slope, and, by comparison with the three previously drilled proximal sites, assess lateral changes in fluid chemistry. A logging suite, including a vertical seismic profile experiment, was performed for optimal correlation between the cores and the seismic data.

A second transect was drilled further south on the margin of the western GBB. The primary objective of the second transect was to assess possible variations in the fluid-flow patterns. Site 1008 (proposed Site F-6) was drilled in 437.1 m of water, and Site 1009 (proposed Site F-4A) in 307.9 m of water. Operational safety considerations required relocating Site 1009 to deeper water than the proposed Prospectus location (F-4). Prospectus Site F-5 was not drilled as a result of operational time constraints.

OVERVIEW

The cores recovered along the Bahamas Transect contain the sedimentary record of sea-level changes throughout the Neogene, and the interstitial water geochemistry provided evidence of fluid flow through the platform margin of the Great Bahama Bank.

Sea-Level Objectives

An extremely exciting result of drilling during Leg 166 is the discovery that the sea-level changes throughout the Neogene can be monitored in the facies successions in the slope sediments of Great Bahama Bank. Facies changes correlated with seismic sequence boundaries and corroborated the interpretation that these sequences are controlled by sea-level changes. Calcareous nannofossils and planktonic foraminiferal biostratigraphical datums were found at all sites and an age-depth relationship was established. The Geomagnetic Polarity Time Scale (GPTS) of Berggren et al. (1995) transferred the biohorizons into time, and the cores were correlated with seismic data by using the time/depth conversion from the vertical seismic profile in each hole. This allowed us to date the sequence boundaries precisely, achieving two of our major sea-level objectives: (1) the facies distribution within the carbonate sequences was documented, and (2) the timing of sea-level changes in the Neogene was established. To compare the sedimentary record of sea-level changes with the oxygen isotope proxy, a basinal hole (Site 1006) was drilled. This core far exceeded our expectations, as most conventional nannofossil and planktonic foraminifers were found in the Pleistocene to middle Miocene section. In addition, recovery was very high and the preservation of the foraminifers was good throughout the recovered section. Thus, all the prerequisites are in hand to establish an oxygen isotopic record of the sea-level changes in the same transect. The correlation of the sedimentary and isotopic record will enable us to assess the causal relationship between sea-level changes and the sequence stratigraphic pattern, thereby fulfilling the third sea-level theme objective.

To achieve these goals the following four data sets were crucial.

1. Lithostratigraphic data

Core recovery was sufficient (55.3%) to document the facies successions throughout the cores (Fig. 3). The facies successions contain indications of sea-level changes on two different scales. First, there are high-frequency alternations of layers containing more platform-derived material with layers containing more pelagic sediments. In the Pleistocene and Pliocene periplatform section, these alternations are reflected in the ratio between neritic components and nannofossils, and mineralogically between aragonite and low Mg-calcite. In previous studies these cycles were shown to correlate to orbitally forced high-frequency sea-level changes in the Quaternary. We found similar decimeter- to meter-scale high-frequency facies changes in the Miocene sections of all the holes. The layers with more platform-derived material are generally lighter in color and are better cemented, whereas the more pelagic layers are darker, greenish, and are less cemented and contain small amounts of clays and silt. Sediments with increased platform input are interpreted to have been deposited during sea-level highstands when the platform was flooded and producing sediment. The sediments with higher siliciclastic input indicate erosion of siliciclastic margins, probably in Cuba and Hispaniola. Because of the color changes and the cementation differences, these cycles are also recorded in color reflectance data and the logs. Formation MicroScanner (FMS) data provided a continuous record of these cycles at two sites, which will be analyzed to determine the frequency of these cycles in the Miocene.

A repetitive pattern of facies succession on the order of tens to several hundreds of meters thick documents the sedimentary record of longer term sea-level changes. These larger-scale patterns are also seen in the seismic images. Similar to the small-scale cycles, changes in the amount of platform-derived material indicate periods of high and low sea level. Platform exposure during low sea level is reflected in reduced sedimentation rates, occasionally leading to hardground formation on the slope. In addition, erosion of the platform margin during these periods is documented by the deposition of coarse-grained packstones and floatstones in pelagic-rich background sediments. Erosional truncation, which leads to hiatuses in the biostratigraphic successions, is also observed in the proximal slope sites. Cycles are best developed during sea-level rises and usually comprise the middle part of the sequences. Redeposition of platform carbonates occurs again in the upper part of the sequences. This pattern is best developed in the Miocene sequences when the platform had a ramp-like morphology. In the Pliocene and Pleistocene, the bulk of the sediments, especially in the more proximal locations, is dominated by thick successions of fine-grained material, but turbidites occur preferentially in the upper parts of the sequences. More mass-gravity flow deposits are found in the distal sites, indicating that the steep upper slopes were bypassed by these flows.

2. Petrophysical and Log Data

To complement the cores and fill in recovery gaps, an extensive logging program was performed in the four deep transect holes. At Site 1003, a dedicated logging hole was drilled when hole conditions prevented the logging of the cored hole. The acquired logs provide detailed information on the sedimentary properties and structure of the strata. Log-to-core correlation permits significant interpretations about variations in sedimentation patterns along the transect sites of GBB from the earliest early Miocene to Holocene. The general compatibility of the discrete data points from shipboard petrophysical measurements with the log data supports the integrity of the data sets. This logging data will help correlate the seismic sequence boundaries to the cores. Over 3 km of Formation MicroScanner data were acquired. These data will allow us to analyze the small-scale cycles observed in the cores and assess their frequency. This analysis has the potential to reveal the frequency of orbitally driven climate and sea-level changes in the Miocene.

For an accurate tie of the cores to the seismic data, vertical seismic profiles with the Well Seismic Tool were acquired in each of the deep holes. These data allowed us to calculate an accurate time/depth conversion of the seismic reflections. These experiments proved to be extremely valuable as neither the integrated log velocity nor the shipboard velocity measurements provided an accurate velocity profile in all the holes. Errors of up to 50 m were obtained using the log or discrete shipboard velocity measurements.

3. Biostratigraphic Data

The most crucial task was to establish the ages of the seismic sequence boundaries and their indicated sea-level changes. Calcareous nannofossils and planktonic foraminiferal biostratigraphic datums were used to establish an age-depth relationship for each of the sites drilled as part of the Bahamas Transect (Sites 1003-1007). Many biohorizons from both micropaleontological groups were identified, establishing a framework of intersite correlation (Fig. 4; Table 1). This framework was transferred into time by using the Geomagnetic Polarity Time Scale (Berggren et al., 1995). This latter step was the most important to obtain absolute ages to fulfill one of the objectives of this leg; testing the age consistency of the sequence boundaries observed in the seismic records and logging data in combination with lithological changes observed in the recovered sedimentary section.

Dating the sediments in upper slope carbonate environments is not always an easy task. At the Leg 166 sites, calcareous microfossils were very rare and difficult to identify in some intervals due to dilution and preservation problems. Fortunately, the boreholes drilled more basinward (Sites 1006 and 1007) contained moderately to well-preserved calcareous microfossils throughout their generally continuous records. Refined biostratigraphies for these holes were established by using the core-catcher samples in the Pleistocene to upper Pliocene sections, and samples from discrete clayey layers in the Miocene sections, which contained moderately preserved calcareous microfossils.

Because Site 1006 is located in the Florida Straits, in a distal position from the platform, it is less affected by diagenetic effects and erosional surfaces associated with sea-level falls than those sites drilled higher on the upper slope. This site, with apparently continuous sedimentation, provides a benchmark for establishing the stratigraphic order of the marker species in this region. Most conventional nannofossil and planktonic foraminiferal biohorizons were found in the Pleistocene to middle Miocene interval at Site 1006. Nannofossil biostratigraphic datums were used exclusively to characterize sedimentation in the Pleistocene section of this site, while the Pliocene and Miocene sections were constrained by both planktonic foraminiferal and nannofossil events.

The depths of planktonic foraminiferal and nannofossil datum levels at Site 1006 were consistent with the relative order of these events in tropical regions except for a few cases. One important mismatch was the first occurrences of *Globigerinoides conglobatus* and *Globorotalia margaritae* relative to nannofossil events in the same interval. These datums have been assigned ages of 5.7 Ma (Berggren et al., 1985) and 6.4 Ma (Berggren et al., 1995), respectively. Chaisson and Pearson (in press) have subsequently modified the age of *Gs. conglobatus* to be 6.2 Ma in the tropical Atlantic. In either case, both of these events occur below the top of the small *Reticulofenestra* spp. interval at Site 1006, dated as 6.5 Ma (Sato et al., 1991). This relationship was also observed at Site 1007. Using the nannofossils only in Site 1006's uppermost Miocene section to establish the age-depth relationship infers that the first occurrences of *Gs. conglobatus* and *Gr. margaritae* are 6.8 Ma and 7.0 Ma, respectively, in the Bahamian region. The base of *Gs. conglobatus* became an important datum level to identify an upper Miocene hiatus in the upper slope Sites 1003 to 1005, and

1007 (see below).

A second apparent problem in the order of the biostratigraphic datums occurred near the middle/upper Miocene boundary. In tropical settings, the first appearance of *C. coalitus* (11.3 Ma) occurs above the last appearance of *Globorotalia mayeri* (11.4 Ma; Berggren et al., 1995). At Sites 1003 through 1007, *Gr. mayeri* is recorded at the same level or above the *C. coalitus* level. However, it has been shown that the top of the *Gr. mayeri* interval is slightly younger in subtropical regions (Gulf of Mexico, Jamaica, and North Atlantic Site 563) than observed in the tropics (Miller et al., 1994; Zhang et al., 1993). The position of *Gr. mayeri* relative to *C. coalitus* at the Bahamas Transect sites is consistent with this observation.

A third inconsistency in the relative position of the datums involves the first occurrence of *C. floridanus* (13.2 Ma), with respect to the first occurrence of *Globorotalia fohsi fohsi* (12.7 Ma). At Site 1003, the base of *C. floridanus* is above *Gr. fohsi fohsi* but occurs at the top of a slumped interval.

In contrast to Site 1006, unconformities appear in the upper slope sites. The most prominent of these is in the late Miocene, recognized in all slope sites. This unconformity was recognized by the juxtaposition of *Gs. conglobatus* (last appearance datum [LAD])-6.8 Ma) with *D. hamatus* (LAD-8.7 Ma). Also observed at this level was the first appearance of *Globorotalia cibaoensis* (7.7 Ma) and *Globigerinoides extremus* (8.1 Ma). At Site 1007, the upper part of the small *Reticulofenestra* spp. interval (LAD-6.5 Ma) was found above the unconformity, indicating the presence of uppermost Miocene sediments (Messinian). Furthermore, the 16-m interval above the 6.5 Ma level contains poorly preserved nannofossils. Above this zone of uncertainty, the sediments are younger than 4.7 Ma, based on the first appearance of *Ceratolithus rugosus*. It is unclear whether this is the true first appearance or whether it extends further down. Therefore, the interval of poor preservation represents either an interval of very low sedimentation (<1 cm/k.y.) or contains a hiatus that straddles the Miocene/Pliocene boundary. A lithologic break at the base of this interval of poor preservation indicates the presence of a hiatus. At Sites 1003 and 1005, a similar interval of very poor preservation was also found, but it extended well above the unconformity, preventing any age assignment to this interval.

At Site 1007, three erosional surfaces were observed in the Pliocene-Pleistocene section. The top is a modern erosional surface with the uppermost sediments being older than 0.95 Ma. Within the upper Pliocene, an erosional surface is identified based on the co-occurrence of several planktonic foraminiferal events (2.0 to 2.4 Ma). The lower/upper Pliocene boundary is unconformable, based on the juxtaposition of the first appearance of *Globorotalia tosaensis* (3.2 Ma) and *Globigerina nepenthes* (4.2 Ma). These unconformities bound an extensive upper Pliocene drift deposit not observed at the other sites, and they are probably caused by current erosion.

Sites 1003 and 1007 recovered middle and lower Miocene sequences, showing four cycles of alternating sedimentation rates (Fig. 5). At both sites, periods of faster deposition (>5 cm/k.y.) occurred from 11.5 to 13 Ma, 15 to 16.5 Ma, 17.5 to 20.5 Ma, and older than 23 Ma. At Site 1007, slow but continuous pelagic sedimentation (<2 cm/k.y.) occurred from 9.5 to 11.5 Ma, 13 to 15 Ma, 16.5 to 17.5 Ma, and 20.5 to 23 Ma. In contrast, these intervals of reduced sedimentation are represented by hiatuses at Site 1003.

In summary, the overall consistency in the relative position of planktonic foraminiferal and nannofossil datums means that a reliable framework for intersite correlation was established for the Bahamas Transect sites. This framework afforded the opportunity to date the lithologic changes and seismic sequences identified along the transect. Determining the timing of the SSBs and lithologic changes provides the critical information to understand the role of sea-level change and its effect on the development of the Bahamian Platform.

4. Sequence Stratigraphy

Sequence analysis was performed on the seismic data prior to drilling (Fig. 6). Erosional truncations and onlap geometries were used to identify seismic sequence boundaries. These geometrical relationships were best observed farther east along the buried platform margins of Great Bahama Bank. The reflections identified as sequence boundaries were traced to the slope and basinal areas of the Leg 166 Bahamas Transect sites. Tracing the reflection horizons is straightforward for the Pleistocene and the lower and middle Miocene sequences. Uncertainties exist for the upper Miocene and lower Pliocene sequence boundaries because the multiples and diffractions generated by the steep GBB margin could not be completely removed. We identified 17 sequences in the Neogene section, which we labeled a-i and k-q, and the basal seismic sequence boundaries were labeled A-I and K-Q. Most of the sequence boundaries are conformable at the Leg 166 sites; however, truncation is observed in the more proximal sites.

The time/depth conversion allowed us to correlate the sequence boundaries to the cores. All sequence boundaries coincide within seismic resolution of about 10 m, with a facies change indicative of a sea-level change. The exact position of the boundaries is recorded on the log data, which has a better resolution than the seismic data. The age at the correlative depth was calculated using biostratigraphic datums and extrapolating sedimentation rates between datums. Although this procedure carries the uncertainty of both the exact position of the biostratigraphic datums and the seismic resolution, the sequence boundaries showed consistent ages along the seismic reflections (Fig. 7). This result is exciting as it confirms one of the major assumptions of sequence stratigraphy: that seismic reflections are time lines.

The ages of the sea-level changes in the Neogene were estimated from the ages of the sequence boundaries. At the proximal sites, where several of the sequence boundaries are associated with erosion that occasionally is detected by a hiatus, the age of the boundaries were taken from the distal conformable locations. In light of the resolution problem, the ages of the sequence boundaries probably have an error bar of approximately 0.2 m.y (Table 2). Nevertheless, the ages indicate that the seismic sequences along the Bahamas Transect record most of the known major (third-order) sea-level changes in the Neogene. Shore-based log-seismic correlation and detailed biostratigraphic analysis will refine the age model for these sea-level changes.

Evidence for Fluid Movement through the Margin of Great Bahama Bank

One of the primary objectives of Leg 166 was to investigate the possibility of fluid-flow processes through the margin of Great Bahama Bank. The association of the fluid chemistry and heat-flow sampling program with the sea-level objectives means that changes in fluid chemistry can not only be examined as a function of age and depth, but also within a sequence stratigraphic framework. This approach is therefore fundamentally different from other investigations of pore-water profiles along carbonate platforms which, in most instances, only drilled single holes.

The clearest evidence for active recharge of fluids through the margin of GBB is derived from the non-steady state profiles of both conservative and non-conservative elements in the upper 100 mbsf pore-water profiles obtained from both the northern (Sites 1003-1007) and southern transects (Sites 1008-1009). A zone was identified (the flushed zone) that is confined to the upper 40 mbsf in which there is an absence of geochemical gradients in both conservative and non-conservative constituents (Figs. 8, 9). The geochemical data in this interval shows essentially no change from bottom seawater concentrations for all of the normally measured cations and anions. The flushed zone at Sites 1006 and 1007, which are situated farther from the platform, is reduced in thickness and exhibits small, but nevertheless significant, increases in Sr^{2+}. A similar upper flushed zone, approximately 40 m thick, also is observed at the sites drilled along the more southerly transect. Most of the sites also showed irregular temperature profiles in this part of the sedimentary column. The absence of geochemical gradients and the irregular temperature profiles support the notion that there is advection of seawater through this portion of the sedimentary column. The small increases in Sr^{2+} at the more distal sites indicate that fluid flow here is reduced relative to the platform.

Below the flushed zone, there is a sharp change in the concentrations of both conservative and non-conservative elements. The SO_4^{2-} concentration decreases sharply, whereas alkalinity and Sr^{2+} increase. The nature of these gradients is not steady state and reflects depression by a downward-advecting fluid. An unexpected finding at all sites was the increase in Cl^- concentration with increasing depth. This increase is probably a result of the diffusion of Cl^- and Na^+ from an underlying brine or evaporite deposits (Fig. 10).

Based on the evidence from the seven sites drilled during Leg 166, there is clear evidence that a mechanism exists, which produces active exchange between the upper 40 m of sediments and the bottom waters. At the present time we do not know the precise mechanism involved in the flushing, only that it exists. The observations are, however, consistent with water being drawn into the platform by the mechanism known as Kohout convection (Kohout, 1967). In this mechanism the temperature difference between the platform interior and the adjacent seaways causes underpressure to develop within the platform, which draws water through the flanks of the platform.

RESULTS

Site 1003

Site 1003 (BT-2/F-2), is one of five sites of a transect that connects the shallow bank with the deeper water areas. Site 1003 is located on the middle slope of the prograding western margin of Great Bahama Bank approximately 4 km from the platform edge and 12.6 km from the borehole, Clino, drilled on the banktop from a self-propelled jack-up barge.

A thick Neogene section (1300 m) was cored at Site 1003. The strata consist of a series of mixed pelagic and bank-derived carbonates with a carbonate content of 92-97%. In the lower Miocene section (Unit VII), a small amount of fine-grained siliciclastics are admixed in the pelagic intervals. The bank-derived sediments occur in pulses, indicating variations of sediment production on the adjacent platform. Foraminifer and nannofossil biostratigraphy yielded precise ages for the lithologic units. Within the Miocene section there are four hiatuses, ranging from 4 to 1 m.y. in duration. Comparison of the lithostratigraphic unit boundaries and the biostratigraphic breaks correlate well with seismic sequence boundaries previously identified in the prograding slope section. Furthermore, the biostratigraphic data confirm the ages of the late Miocene to Pleistocene sequences that were determined in the two core borings, Unda and Clino, on the shallow bank. The good core recovery obtained throughout the entire section at Site 1003 (overall <40%) and the abundance of biostratigraphic markers have made it possible to accomplish two of the primary sea-level objectives. That is, it is possible to define the ages of the Neogene sequence boundaries and to test their consistency with ages determined in the Unda and Clino boreholes, and to retrieve the sedimentary record of the middle- to lower-slope portions of the prograding sequences. Diagenetic alteration in the lower portions of the hole, however, will preclude the establishment of a stable-isotope stratigraphy for the entire Neogene at this site.

Chemistry from interstitial waters yielded interesting depth profiles with abrupt changes across stratigraphic boundaries. These data in conjunction with the temperature profiles support fluid movement in stratigraphically defined conduits.

Seven major lithologic units are distinguished. Each of these units displays a general trend from bioturbated mudstones and wackestones at the bottom to an increase of packstones, grainstones, and floatstones toward the top. Within the units, subdivisions are defined based on the facies types and associations, textures, and the major components.

Unit I (0-162.1 mbsf; latest Pliocene to Holocene) consists of unlithified to partially lithified mudstones, wackestones, packstones, and floatstones. Its base is defined by the sudden appearance of peloids, which are a major component throughout the unit. Two subunits are recognized. In Subunit IA (0-59.9 mbsf), two intervals of unlithified packstones to floatstones, containing *Halimeda* debris and lithoclasts, are intercalated in unlithified mudstones. In Subunit IB (59.9-162.1 mbsf), an upper aragonite-rich part with some laminated redeposited intervals overlays a poorly stratified and bioturbated mud- to wackestone.

Unit II (162.1-368.2 mbsf; early Pliocene) consists of partially lithified, intensely bioturbated wackestones with some variation in bioturbation and skeletal fragments. The unit is slightly dolomitized (20-25%) at the top, decreasing downhole to about 10%.

Unit III (368.2-492.7 mbsf, early Pliocene) has a characteristic succession of facies that is repeated in the underlying units. The top part of this and the following units are dominated by packstones to grainstones that often display sedimentary structures indicative of turbidites and other mass-gravity flow deposits. The background sediment of these packstones and grainstones are bioturbated wackestones. The bottom part of the units are composed of packstone to wackestone alternations of light gray, lithified beds with an average thickness of 30 to 40 cm and darker, greenish to brownish gray, less lithified intervals of 15 to 25 cm thickness. The alternations are moderate to heavily bioturbated and contain planktonic and benthic foraminifers and other bioclasts.

Unit IV (492.7-643 mbsf; middle to late Miocene) is subdivided into two subunits. Subunit IVA (492.7-591.2 mbsf) is dominated by packstones and grainstones, and is characterized by interbedded light gray to grayish laminated, fining-upward beds and greenish to brownish gray, strongly bioturbated beds. Subunit IVB (591.2-643 mbsf) consists of moderately to heavily bioturbated light gray to dark gray, slightly dolomitized bioclastic packstones to grainstones. Components in the packstones and grainstones include planktonic and benthic foraminifers, bioclasts (including rare *Halimeda* debris), and lithoclasts. Subunit IVB is characterized by a cyclic alternation between well-lithified packstones with large well-developed burrows and finer-grained zones with flattened burrows.

Unit V (634-915.8 mbsf; middle Miocene) can be separated into two subunits. Subunit VA (646-738.8 mbsf) consists of laminated, bioclastic packstone and grainstone beds with sharp or scoured bases. Dominant allochems include planktonic and benthic foraminifers. In Subunit VB (738.8-915.8 mbsf) wackestones and packstones grade downhole into mudstones and wackestones that show a distinct cyclicity of light gray, well-cemented, moderately bioturbated intervals, and strongly bioturbated, dark gray to green layers. These darker intervals also contain a small amount of clay- and silt-sized quartz, plagioclase, and clay. Thickness of a total cycle ranges from 50 to 200 cm.

Unit VI (915.8-1151.63 mbsf; early Miocene to middle Miocene) is separated into two subunits. The top of Subunit VIA (915.8-973.38) is characterized by a well-defined, irregular surface (hardground). The subunit has intercalations of packstones and floatstones within background sediment composed of bioturbated, greenish-grayish wacke- and packstones. The background deposits show the same type of cyclicity as Subunit VB. The underlying Subunit VIB (973.89-1151.38) is three times thicker than Subunit VIA and consists entirely of cyclic alternations of lighter and darker intervals as previously described.

In the lower Miocene Unit VII (1151.63-1296.41 mbsf), the packstone dominated Subunit VIIA (1151.63-1194.77) is even thinner (43 m) and its packstones are thin-bedded (5-10 cm). In contrast, the underlying cyclic Subunit VIIB (1194.77-1296.41) is over 100 m thick. In this subunit, the siliciclastic admixture is approximately 5-7%. Units IV-VII, therefore, show an overall thickening and coarsening-upward trend in their packstone-dominated subunits, indicating a pulsed, but progressive progradation of Great Bahama Bank throughout the Miocene.

Dating the Neogene sedimentary packages deposited in an upper bathyal environment on the slope of western Great Bahama Bank was possible, despite problems of diagenesis and dilution. Most of the conventional Neogene nannofossil and planktonic foraminifers datum levels used in the deep-sea pelagic environment were also found here, and a fine nannofossil-planktonic foraminiferal stratigraphy was established. The sediments recovered at Site 1003 yielded a large number of biohorizons, both from calcareous nannofossils and planktonic foraminifers appearing in proper succession, which is remarkable given the nature of the sedimentary sequence close to the bank. The onset of modern platform production is documented by a high-sedimentation rate during the last 0.9 to 1.0 Ma (10 cm/k.y.). The lower Pleistocene to upper Pliocene interval shows a much slower sedimentation rate of about 2.5 cm/k.y., indicating a decreased input from the banktop. The lower Pliocene section (Units II and III) is an expanded section. During this period of time, the platform produced a lot of material that was shed onto the upper slope. In contrast, the early late Miocene is characterized by pelagic sedimentation rates of about 3 cm/k.y. This was a time of global cooling and falling sea level that ultimately caused an unconformity, separating the lowermost upper Miocene from the lower Pliocene. This unconformity coincides with the lithologic break between sedimentological Units III and IV. In general, the middle Miocene shows a very high sedimentation rate of up to 15 cm/k.y. One unconformity was identified within this interval; planktonic foraminiferal Zones N9 and N10 are missing. The unconformity coincides with the hardground that marks the top of Unit VIA. The lowermost unconformity separating lithological Unit VIIA from Unit VIIB occurs within nannofossil zone NN2 and straddles the planktonic foraminiferal Zones N4 and N5. The Miocene unconformities punctuate periods of high sedimentation rates during which the input from the platform must have been high.

Sedimentation from the lowermost Miocene to the Holocene seems to be controlled by changing sea level. Thick and expanded upper and middle Miocene intervals coincide with the generally high sea level of this time. The late Miocene, a time of global cooling and sea-level fall, is recorded in the sediments as a reduced interval and a subsequent hiatus. The Pliocene sea-level rise resulted in renewed flooding of Great Bahama Bank and sedimentation on the slope. The sedimentary successions of more pelagic deposits alternating with more neritic sediments provide evidence of the numerous sea-level changes during the Pliocene and Pleistocene. These sea-level controlled sedimentologic variations are recorded on the seismic data as well. With one exception, all the sequence boundaries determined prior to drilling coincide either with unit or subunit boundaries. Two unit boundaries occur within seismic sequences indicating a higher resolution within the sedimentary record. In addition, small-scale sedimentary cycles provide evidence for high-frequency sea-level changes.

The carbonate mineralogy is dominated by aragonite with lesser amounts of high-magnesium calcite (HMC) and dolomite throughout the upper 110 mbsf. Below this depth, corresponding approximately with the Pliocene/Pleistocene boundary, aragonite decreases markedly, HMC disappears, and dolomite becomes more important. Variable amounts of dolomite are present throughout the remainder of the core, commonly occurring below nondepositional surfaces. Small amounts of feldspar are also present in the lower portion of Hole 1003B. Diagenetic minerals such as celestite, elemental sulfur, and chert are found sporadically throughout, particularly in fractures. Carbonate contents are generally high throughout the samples measured, and organic contents are generally low. In the Miocene section, however, carbonate content gradually decreases to 85% and drops to 50% or less in the intervals above sequence boundaries, providing further evidence of reduced carbonate input in these intervals. The packstones to wackestones between 700 to approximately 1000 mbsf in Hole 1003C, possess a strong petroleum odor and have experienced some oil migration.

The pore-water chemistry shows very unusual trends, which are probably related to lateral movement along more permeable sedimentary units. Although there are gradual changes in most chemical constituents with increasing depth, these changes accelerate across major permeability barriers. The shallowest of these changes occurs at around 85 mbsf. Below this depth, the salinity starts to increase, reaching values as high as 62 at 820 mbsf. Alkalinity and H_2S also increase across this barrier while sulfate decreases. Calcium continues to increase throughout the hole while the relative concentration of Mg decreases. Nonsteady-state profiles exist for all of the measured constituents (salinity, SO_4, Ca, Sr, NH_4, Li, F, alkalinity, and Mg). The C_1/C_{2+} ratio was considered to be anomalous throughout the hole indicating the presence of migrated hydrocarbons. Alkanes higher than C_2 first appeared below a major change in velocity at 750 mbsf, which, in addition to being a seismic reflector, was also a seal. It is probable that the hydrocarbons and bitumen found in the core were generated deep in the section and migrated upward and laterally. As these compounds moved upward they were oxidized by sulfate-reducing bacteria to produce H_2S and consequently lower pH. Decreases in the pH promote the extensive carbonate alteration seen throughout the core.

The log data obtained from Hole 1003D correlate well with the sedimentary succession and can be used to fill in gaps in low recovery zones. With log-to-core correlation, the changes recorded in the logs can be traced along the seismic sequence boundaries, providing a tie of the sedimentation patterns at Site 1003 to other drill sites across the Great Bahama Bank platform margin and on the platform top. A general downhole trend of increasing density, resistivity, and sonic velocity, and of decreasing porosity probably results from sediment compaction. However, there is a pronounced change in this trend at 738 mbsf, where the downhole gradient in density, resistivity, and velocity is offset toward lower values while the porosity increased. This anomalous pattern may be the result of changing sediment composition as well as a diagenetic overprint. Below 738 mbsf, this major lithology change is apparent in the natural gamma-ray and geochemical (Ca, Al, and Si) logs. The increased frequency and magnitude of the uranium signal is particularly notable. The salinity indicator ratio in the geochemical logs shows a sharp increase below 738 mbsf, implying a more saline formation fluid, which is consistent with the high chlorinity measured in pore waters from these depths. Also below 738 mbsf, a notable cyclicity in the gamma-ray and FMS logs correlates to the sedimentation patterns noted throughout much of the Miocene portion of the cores.

Site 1004

The primary objective of Site 1004 is to obtain heat flow and interstitial water geochemistry measurements to be used in conjunction with data obtained from Sites 1003, 1005, 1006, and 1007 to ascertain possible fluid flow and diagenetic reactions in the carbonate margin. In addition, this site serves as a location for the study of high-resolution sea-level changes during the Pleistocene, as well as providing additional information for the broader sea-level objectives of Leg 166.

A Pliocene-Pleistocene section (200 m) was drilled at Site 1004, which is located on the slope of Great Bahama Bank. The strata consist of a series of mixed pelagic and bank-derived carbonates with a carbonate content of 92-97%. Adara and WSTP temperature measurements confirm the presence of a non-steady state temperature profile suggesting an inflow of water into the slope sediments. Pore-water geochemistry and gas analyses show an extremely active diagenetic zone between 110 and 200 mbsf with alkalinity values as high as 70 mM, depletions in Mg and Ca, and enrichments in Sr. This zone corresponds with high concentrations of methane and hydrogen sulfide. Hydrogen sulfide readily degassed from the cores between 50 and 135 mbsf as soon as they were brought to the surface.

One major lithologic unit was distinguished. Unit I (0-200 mbsf; latest Pliocene to Holocene) is equivalent to Unit I described in Site 1003. It consists of several 5-to-10-m-thick intervals of light-colored, unlithified to partially lithified peloidal wackestones to mudstones, which alternate with thin 0.5 to 1 m intervals of gray, partially lithified wackestones to packstones, grainstones, and floatstones. Subunit IA (0-81.1 mbsf) contains multiple oscillations between zones of coarse, blackened grains with lithoclasts and fine periplatform ooze. Subunit IB (81.1-200 mbsf) contains an overall coarsening-upward sequence of partially dolomitized mudstones and wackestones with some coarser grained intervals.

Sediments recovered from Hole 1004A provide a record for the Pleistocene through the uppermost Pliocene, although the abundance and preservation of both nannofossils and foraminifers vary throughout the recovered sequence. The sedimentation rate is high throughout the Pleistocene, and modern platform production and shedding began to influence this site much earlier than the more distal site, Site 1003. Throughout Subunit IA, a number of alternations in sediment composition, color, and mineralogy can be recognized that probably correspond to sea-level changes. Lowstands are characterized by higher concentration of low-Mg calcite and darker color compared to highstands which contain abundant aragonite and high-Mg calcite. Below the bottom of IA, these cycles can no longer be recognized because of poor core recovery and the influence of diagenesis. The main effect of diagenesis is the dissolution of aragonite and HMC and the formation of low-Mg calcite (LMC) and dolomite.

Based on pore-water geochemistry, two distinct geochemical zones were identified at Site 1004. An upper zone, extending from the seafloor to a depth of 40 mbsf, is characterized by an absence of significant changes in the interstitial pore-water geochemistry. Geothermal measurements also indicate a reduced temperature gradient in this interval, suggesting the influx of seawater. The upper zone gradually merges into a region with salinity between 45 and 50, below 110 mbsf. In this lower region, concentrations of both Ca and Mg are depressed and Sr is elevated. This region corresponds to high concentrations of CH_4 (up to 20,000 ppm) and H_2S (up to 21,000 ppm). Although the C_1/C_2 ratio was over 2000 in this region, there were still detectable concentrations of C_3 and C_4 gases.

Site 1005

Site 1005 is the most proximal of the five sites that constitute the Bahamas Transect. Site 1005 is located in 352 m of water, approximately 1150 m from the modern platform edge on the upper slope, 30 shot points SW of the crossing of seismic lines 106 and 107. It is positioned on the thickest portion of the prograding Neogene sequences seen on the seismic line. The target depth of 700 m was designed to penetrate seven seismic sequences. The sea-level objectives of Site 1005 were (1) to date precisely the sequence boundaries; (2) to determine the facies within the different systems tracts, especially the nature of the onlapping units that were interpreted as lowstand deposits; and (3) retrieve a high-resolution record of climate and sea-level fluctuations for the Quaternary and late Pliocene. This site served also as the proximal site for the fluid-flow transect. A logging suite was collected to provide a continuous record of the sedimentary succession. In addition, a vertical seismic profile (VSP) was shot for an accurate time-depth conversion of the seismic reflections, so that the cores could be correlated precisely to the seismic data.

A 700-m-thick upper middle Miocene to Holocene section was recovered at Site 1005. The sedimentary succession consists of a periplatform sedimentary section of mixed pelagic and bank-derived carbonates, with a carbonate content of 72-99%. The section is comprised of unlithified to partially lithified wackestones and slightly coarser grained intervals consisting of packstones and grainstones. Compositional variations document an alternating pattern of bank flooding, concomitant shedding to the slope with periods of exposed banks, and a shutdown of shallow-water carbonate production and largely pelagic sedimentation that is recorded in alternating high and low sedimentation rates. The pulses of bank-derived material coincide with the prograding pulses observed on the seismic data that were interpreted to be seismic sequences. This indicates that sea-level changes exceed the major control on the development of the seismic sequences. Foraminifer and nannofossil biostratigraphy yielded precise ages of the lithologic units and seismic sequence boundaries. One of the seismic sequence boundaries coincides with a hiatus that probably straddles the Miocene/Pliocene boundary. Three other boundaries correlate to changes in sedimentation rates, whereas a biostratigraphic hiatus was not detected with the remaining boundaries. The biostratigraphic data from Site 1005 confirm the ages that were carried along seismic reflections from Sites 1003 to 1005. This consistency gives a first indication that the seismic sequence boundaries along the Bahamas Transect are indeed time lines. The cores, in combination with the logging data, provide the facies information in the seismic sequences and systems tracts. Fewer mass-gravity flow deposits are present than at Site 1003, indicating most of the platform-derived turbidites bypassed the upper slope. The thick Quaternary section is characterized by sedimentation cycles with all the characteristics of the periplatform aragonite cycles found in the basin surrounding the Bahamian platforms. These cycles are interpreted to have formed as a result of the high-frequency Quaternary sea-level changes.

As observed at Sites 1003 and 1004, pore-water chemistry profiles at Site 1005 display normal seawater concentrations of all constituents in the upper 45 mbsf, indicating rapid exchange with the water column. Below this zone, organic matter remineralization reactions dominate the diagenetic changes. These reactions are a result of the high in situ abundance of organic material trapped within these marginal sediments during rapid Pliocene-Pleistocene platform shedding events, and provide the fuel that drives the early carbonate alteration reactions in these shallow sediments. Below 400 mbsf, increased salinity suggests the presence of deep-seated saline fluids. Positive salinity anomalies between 50 and 150 mbsf suggest that some of the fluid is derived from the platform surface.

The sedimentary succession of Site 1005 can be subdivided into four units. Although these sediments were deposited in a proximal position on the slopes of GBB, they are generally fine-grained. Their main components are aragonite mud, platform-derived skeletal debris, and pelagic foraminifers and nannofossil ooze.

The basal boundary of Unit I (0-261.7 mbsf; late Pliocene to Holocene) is placed at the onset of peloids and aragonite mud. Variations in abundance of these two components were used to further subdivide the unit. Only a few turbidite layers are preserved as a result of heavy bioturbation that obliterated many primary sedimentary structures. The sediments consist of unlithified to partially lithified mudstones, peloidal wackestones, and packstones. Components in the silt and sand fraction are peloids, benthic foraminifers, *Halimeda*, and other skeletal debris. Unit IA shows a cyclic-sedimentation pattern with aragonite intervals alternating with more pelagic intervals. Turbidites are concentrated in the aragonite intervals. Subunit IB is partially dolomitized and has a similar composition, but it does not display the pronounced cyclicity of Subunit IA. Subunit IC is also slightly dolomitized and consists mostly of partially lithified mudstones and wackestones with thin layers of clay- to silt-sized laminated intervals. The silt-rich layers are enriched in pelagic and benthic foraminifers, and pellets.

Unit II (261.7-360.9 mbsf, early Pliocene) is a homogeneous section of partially lithified and dolomitized mudstone to wackestones. The constituents are predominantly pelagic foraminifers, with minor amounts of benthic foraminifers, lithoclasts, and unidentifiable bioclasts.

In Unit III (360.9-534.3 mbsf, early Pliocene to late Miocene), aragonite needles or pellets are no longer observed. The succession of partially dolomitized foraminifer wackestones displays a cyclic pattern. Gray to light-gray, well-cemented biowackestones alternate with less cemented gray to olive-gray wackestones with compacted burrows. The boundary between the two lithologies is generally sharp. The average thickness of the compacted intervals in this unit is approximately 44 cm, but is thickest in the bottom portion of the interval.

In the middle to upper Miocene Unit IV (534.3-700 mbsf), a cyclicity similar to Unit III is observed, however, the compacted interval of the cycles is nearly 80 cm thick. The top of Unit IV is marked by a series of thin-bedded turbidites that are intercalated in the cycles. The cycles are interpreted as being formed by variations in the amount of platform-derived material from the slope. The gray, well-cemented intervals have a higher abundance of platform-derived clasts, whereas the darker layers contain more planktonic foraminifers and have a higher organic content.

The cores recovered at Site 1005 document that the upper slope environment of the prograding margin of GBB is dominated by fine-grained sediments. The variations in these mudstones and wackestones are subtle, but nevertheless give a record of high-frequency cyclicity of platform shedding as a result of high-frequency sea-level changes. The observed trend of increasing thickness of the gray lithologies of the cycles within Units III and IV indicate an increase of progradation in these units.

Although Site 1005 was only 1.5 km from the modern platform edge of GBB on the upper slope, biostratigraphic dating was possible, and there was good agreement between the nannofossil and planktonic foraminiferal biostratigraphic events. Biostratigraphy indicates continuous sedimentation from the Pleistocene to the lower Pliocene. A major hiatus occurs across the Miocene/Pliocene boundary that spans from 5.6 to 8.6 Ma. A hiatus of similar duration was also found further downslope at Site 1003. In the previously drilled shallow-water platform sites Unda and Clino, the hiatus is not as extensive as more of the upper Miocene section is preserved. At Site 1005, the faunal assemblages below this unconformity are early late to late middle Miocene in age.

The benthic foraminiferal assemblages indicate an upper bathyal paleodepth for Site 1005. The diversity and abundance of platform-derived benthic foraminifers provide an additional record of platform progradation and flooding events. In much of the Pleistocene section, there is a diverse and abundant benthic fauna, whereas a depauperate assemblage is found in the late Pliocene. In the early Pliocene and the Miocene, a low-diversity, shallow-water assemblage is diluted in the monotonous sediments.

Variations in sedimentation rates reflect the export of bank-derived material to the upper slope. The late Pleistocene sedimentation rate is high (15 cm/k.y.), but it is reduced during the late Pliocene and early Pleistocene (3.5-1.2 Ma) to approximately 2 cm/k.y. This latter rate is characteristic of normal pelagic carbonate sedimentation with little to no addition of platform-derived material. The lower Pliocene sedimentation rate was again high (10 cm/k.y.), indicating that the leeward side of GBB received large amounts of platform-derived material during this period. A hiatus that spans nannofossil zone NN11 (5.6-8.6 Ma) was probably caused by the combination of large-scale slope erosion associated with lower sea level and increased current activity, as there is little to no pelagic sedimentation recorded. An expanded lower upper Miocene section was recovered below the hiatus. The high sedimentation rate of 11 cm/k.y. during nannofossil zones NN9 and NN10 reflects another period of platform shedding, consisting mostly of fine carbonate mud to the upper slope. There is minimal input from the platform during nannofossil zone NN8. Another high input of platform derived material occurred during the late middle Miocene yielding sedimentation rates of 13 cm/k.y. The sedimentation rates are in concert with long-term sea-level changes. The two largest known sea-level falls straddle the middle/late Miocene and early/late Pliocene boundaries and are clearly expressed in the sedimentation rates at Sites 1005 and 1003.

A check shot survey (VSP) was performed that enabled us to correlate the cores to the seismic data. The seismic sequence boundaries correlate well with the biostratigraphic data. Three of the six sequence boundaries coincide with changes in sedimentation rates and the late Miocene hiatus falls exactly on a sequence boundary. In addition, the thick seismic sequences coincide with the periods of high sedimentation rates. There is also a good correlation of the seismic sequence boundaries with the changes in mineralogy. In the Pleistocene section, the sequence boundaries coincide with intervals with lower percentages of high-Mg calcite and aragonite that record reduced platform-derived sediment input. In the Pliocene and Miocene section, the boundaries are either associated with high amounts of insoluble residues or peaks of dolomite. The overall monotonous sediments do not change dramatically at sequence boundaries, but they generally correlate to mudstone intervals that contain a larger amount of nannofossil ooze. The oldest sequence boundary recovered in the middle Miocene is marked by a firmground. The log data correlate well with the seismic sequence boundaries. Not surprisingly, the velocity profile has the strongest correlation.

The log data correlate well with the sedimentary succession and can be used to fill in gaps in low-recovery zones. The strong cyclic nature of the data is the most notable feature recorded in all the logs, specifically from 700 to 385 mbsf (middle Miocene to lower Pliocene) and from 260 to 90 mbsf (upper Pliocene to Pleistocene). The intervening section from 385 to 260 mbsf (lower Pliocene) is marked by an apparent stark diminution of the intensity of the cycles, as reflected in particular by the regularity of the resistivity curve. Between 260 to 90 mbsf, the sharp increases in gamma-ray intensity correlate with increased density, resistivity, and velocity and decreased porosity. This association is indicative of more indurated sediment deposited during periods with a reduced sedimentation rate leading to hardground formation. The logs clearly display that sedimentation was punctuated by periods of decreased sediment input that are marked by the formation of better cemented layers.

In summary, the sedimentary, mineralogical, geophysical, and stratigraphic data record a sedimentary system characterized by variable input of platform-derived sediment that is most likely caused by changing sea level. These fluctuations of input occur on several levels. A high-frequency, cyclic alternation is seen in the sedimentary and log data, whereas the sedimentation rates monitor the long-term changes. The seismic sequences reflect these long-term changes and also provide a record on an intermediate scale.

The interstitial water chemistry at Site 1005 yielded interesting geochemical profiles that were subdivided into four zones. The top 45 mbsf, zone 1, displays no change in most measured constituents. This zone probably experiences pervasive flushing of seawater that prevents diffusional gradients from developing between the overlying seawater and the underlying saline fluid. Zone 2 extends to a depth of 190 mbsf and is characterized by a sharp change in the gradient of all major and minor pore-water constituents. Cl^- is enriched in this zone, which is interpreted to be an intrusion of saline, sulfate-rich water derived from the shallow platform. High rates of microbial sulfate reduction within this zone reduce the sulfate concentration to zero and give all major ion profiles an anomalous appearance. Most constituents in the underlying zones 3 and 4 display a steady change to the bottom of the hole. A shift in many of the profiles marks the boundary between zone 3 and 4. At this time it is not known to what extent the shifts are influenced by diagenetic alterations within lithological units or fluid flow within these boundaries.

The cores and data collected at Site 1005 provide the necessary information to answer several of the questions addressed before drilling this site. In regard to the sea-level objectives, the data corroborated the results of the more distal Site 1003. Site 1005 also yielded abundant biostratigraphic markers that allow for the precise age dating of sequence boundaries. Furthermore, the ages can be carried along the seismic reflection horizons to Site 1003 where they fall on the same stratigraphic level. This consistency documents that the seismic reflections are indeed also time lines and have a chronostratigraphic significance. This is possible because the impedance that causes seismic reflections is controlled by both original sediment composition and the diagenetic overprint. In these carbonate slope sediments, sediment composition itself is largely controlled by the input of platform-derived sediment, which in turn is related to sea-level fluctuations. Early diagenetic alteration was strongest when the platform was exposed and sedimentation rates were reduced. Thus, both facies and diagenesis are related to sea-level fluctuation, which leaves its expression in physical properties and finally in the seismic sequences.

In regard to the fluid-flow objectives, the geochemical profiles of Site 1005, in conjunction with Sites 1003 and 1004, provided further evidence for fluid flow through the slope of GBB. The consistency of changes in geochemical gradients at distinct stratigraphic horizons indicate that the flow has a horizontal component in the upper sediments that is superimposed on the vertical diffusion in the lower portions of the sedimentary column.

Site 1006

Site 1006 is located in 650 m of water approximately 30 km from the western platform edge of Great Bahama Bank. It is the most distal of the five transect sites positioned at the crossing of seismic lines 105 and 106. Drilling at Site 1006 was designed to core and log a thick sequence of drift deposits that were thought to extend through the Neogene with relatively few hiatuses. There were two principal objectives at this site. First, the sediments at Site 1006 were believed to have a greater pelagic component than the more proximal transect Sites 1003, 1004, 1005, and 1007. Therefore, they were more likely to be well suited for dating and establishing an oxygen and strontium isotope stratigraphy for the Neogene, thereby providing an independent indicator of sea level. Using the sequence stratigraphic framework, these datums could then be traced on the seismic reflections to the distal lobes of the prograding margins at the proximal sites. This approach will aid in the dating of the proximal sites where the chronostratigraphy is occasionally unclear as a result of missing sequences, poor recovery, diagenesis, and/or dilution by neritic sediments. The second objective was to determine if changes in the composition of the sediments varied in conjunction with variations in the strength of the Florida Current. If so, we will be able to correlate these variations with changes in sea level as recorded by the prograding and regressive sequences at the platform sites and the oxygen isotopic signature of the foraminifers.

A final objective was to examine pore-water chemistry in a more basinward site where pore-water and geothermal gradients, in contrast to the slope sites, were believed to be predominantly diffusive in nature and not influenced by fluid flow.

A 717.3-m-thick middle Miocene to Holocene section was recovered at Site 1006. The sedimentary section consists of mixed pelagic and bank-derived carbonates with varying amounts of clay material believed to have been derived from Cuba and Hispaniola. The biostratigraphic control throughout Site 1006 is very good and almost all planktonic foraminiferal and nannofossil zones from the Pleistocene to upper middle Miocene are found. The abundant pelagic biogenic components are less diluted by platform-derived material, and microfossil preservation is less affected by diagenesis than in the upper slope sites (Sites 1003, 1004, and 1007). Benthic foraminifers indicate an upper middle bathyal paleodepth. An excellent record of magnetic susceptibility exists, showing fluctuations between negative and positive values that reflect the input of clay material. A magnetic reversal was found between 4.5 and 6.0 mbsf which was tentatively correlated with the Blake event (0.13 Ma). Good agreement was found between the integrated sonic and VSP logs and the calculated depth of the sequence boundaries. Chemical profiles reveal a shallow flushed zone extending to 30 mbsf. Below this depth, profiles are mainly diffusionally controlled with the exception of certain elements which are locally influenced by diagenetic reactions.

Sediments were divided into five lithostratigraphic units on the basis of compositional and textural changes. Unit I (0-125.95 mbsf, Hole 1006A; 0-127.9 mbsf, Hole 1006B; Pleistocene to late Pliocene) consists of largely unlithified, bioturbated nannofossil ooze (sand to silt-sized foraminifers) with a small component of aragonite needles in Subunit IA. Particle abundance and grain size increase downhole to the base of the subunit. In Subunit IB this ooze is interbedded with gray and olive clays reflecting erosion of siliciclastics from Cuba and/or Hispaniola.

Unit II (125.95-360 mbsf, Hole 1006A; 127.9-176.5 mbsf, Hole 1006B; Pliocene to early Pliocene) consists of nannofossil ooze and chalk in which some grains were infilled as a result of pyritization. In Subunit IIA there is an alternation between nannofossil ooze and a more aragonite-rich ooze containing some peloids. Subunit IIB is defined by the occurrence of chalk, but is generally very uniform as a result of the high rates of sedimentation. Minor to moderate bioturbation is pervasive.

Unit III (360-528.7 mbsf; early Pliocene to late Miocene) is composed primarily of light gray and light greenish-gray chalk. The unit consists of a series of fining-upward intervals. Firmgrounds characterized by sharp burrowed contacts are frequent in the upper part.

Unit IV (528.7-594.25 mbsf; late Miocene to latest middle Miocene) is composed of light gray and greenish-gray nannofossil chalk. The uppermost portion contains a series of thick intervals with sharp basal contacts. Within each interval, nannofossil chalk with bioclasts grade upward into nannofossil chalk and clay. The lower part of the sequence is punctuated by a series of firmgrounds.

Unit V (594.25-717.3 mbsf; middle Miocene) is composed of alternating intervals of olive nannofossil chalk and light gray nannofossil chalk with foraminifers. Throughout the entire unit, no primary sedimentary structures are visible. The degree of lithification increases downhole with the result that the lower portion consists of alternating intervals of chalk and limestone. The greenish gray to olive intervals are characterized by well-defined, flattened burrows that occur in association with *Chondrites*-type burrows. The light-gray intervals contain larger, well-defined burrows.

The facies succession at Site 1006 is interpreted as being governed by an interplay of current activity and sea-level fluctuations. We suggest that the bottom of cycles, which contain clay intervals, reflect the erosion of siliciclastics. These are overlain by nannofossil ooze with platform-derived bioclasts corresponding to neritic production. The uppermost stage consists of nannofossil ooze and planktonic foraminifers. These changes are reflected in the bulk mineralogy, with high aragonite recording high sea level. Aragonite content also appears to be highly correlated with the color reflectance at the 700-nm wavelength.

All nannofossil and planktonic foraminiferal zones were present throughout the middle Miocene to Pleistocene section. The lower Pliocene section of the sequence is expanded with foraminifers showing little evidence of diagenetic alteration, and it is ideal for paleoceanographic studies. An excellent record of magnetic susceptibility, which is suspected to be tied to changes in the clay content of the sediments, is present throughout the upper Neogene. A magnetic reversal was found between 4.5 and 6.0 mbsf, which was correlated with the Blake event (0.13 Ma).

Sedimentation rates vary considerably at Site 1006. The rates can be divided into four distinct periods. The rate for the Pliocene-Pleistocene section is 5 cm/k.y., which is considerably lower than the same interval at Sites 1003-1005. The rate for the lower Pliocene and uppermost Miocene sections is 12 cm/k.y., similar to the proximal sites, suggesting that similar depositional processes were influencing the sites during this period. The upper Miocene interval has a low sedimentation rate (3 cm/k.y.) that is within the range of normal pelagic sedimentation. The middle Miocene section has slightly higher rates, perhaps because of contourite deposition and the deposition of fine-grained, platform-derived material.

The predicted positions of the sequence boundaries using velocities calculated from the integrated sonic log and vertical seismic profile showed excellent agreement with the multi-channel seismic data. These boundaries fell in the expected positions based on correlations determined at Site 1003. Measured discrete velocities, however, predicted significantly lower interval velocities, a phenomenon resulting from the soft nature of the rocks and the fact that shipboard velocities are not measured under in situ pressure.

A full suite of logs, with the exception of the Geochemical Logging Tool (GLT), was run from 103 to 716.8 mbsf. Throughout the entire sequence, the logs were characterized by small-scale cyclicity observed as alternations between thin, resistive, low natural gamma-ray layers and conductive layers with higher gamma-ray counts. The cyclicity is also well defined by porosity, density, and velocity. Firmgrounds are recognized by increased gamma-ray, resistivity, and sonic velocity. A pattern of larger-scale cyclicity reflects changes in the abundance and spatial frequency of the cycles. These patterns may be related to depositional changes associated with current intensity and can be tentatively correlated with sequence boundaries. As a result of the high-percentage core recovery, these logs offer an excellent opportunity for core-log correlation.

The mineralogy at this site is dominated by low-Mg calcite. Aragonite is abundant in the

Pleistocene age sediments decreasing to less than 5% in the upper Pliocene sequence. The concentration of aragonite increases to 40% in upper Miocene sediments. High-Mg calcite is present in the uppermost 20-30 mbsf, but quickly disappears coincident with the presence of dolomite. Dolomite is a minor but ubiquitous component throughout the core. With the exception of the upper 30 mbsf, the sediment profiles are dominated by diffusion from an underlying brine with local reactions involving Ca, Mg, Sr, K, Li, F, and Si providing deviations from the ideal diffusive profiles. In the upper 30 mbsf, there are no gradients in the major elements and only very small increases in alkalinity and Sr. Below this depth Cl^- increases steadily to the base of Hole 1006A reaching a concentration of 717 mM. The Sr concentration increases steadily over this interval as a result of the dissolution of aragonite and the precipitation of calcite and dolomite. At 452.95 mbsf the Sr concentration reaches 7 mM, the highest values recorded in ODP or Deep Sea Drilling Project (DSDP) history. The Sr can attain this high concentration primarily because sulfate has been completely utilized in the oxidation of organic material. Concentrations of H_2S are low at this site as a result of the abundance of iron which allows the formation of pyrite.

In summary, Site 1006 has met and exceeded all its initial expectations. Based on shipboard biostratigraphy, the sequence boundaries were dated and traced to the proximal sites where the ages agree well with those determined at Sites 1003 and 1005. The position of the boundaries was verified using a combination of VSP and integrated sonic logs. The excellent, continuous sedimentary sequence contains abundant well-preserved foraminifers, which will be dated using O- and Sr-isotope stratigraphy and tied to the shallow sites to date sea-level changes. In addition, the O-isotope stratigraphy provides its own independent record of sea-level changes. This correlation allows another primary goal of Leg 166 to be achieved; the isotopic and sedimentary record can be compared. The expanded Pliocene and upper Miocene sequence combined with the excellent microfossil preservation will allow this site to become a classic site for upper Neogene paleoceanography in the low-latitude Atlantic.

Site 1007

Site 1007, at the crossing of seismic lines 106 and 102B, is located on the toe of the western Great Bahama Bank slope in 647 m of water. The target depth was the base of the Neogene, which was estimated to be at approximately 1230 mbsf. The site is positioned to penetrate the thin basinal portions of 16 prograding sequences and, in the upper part, a thick onlapping wedge that could be either a drift deposit or an accumulation of mass-gravity flows. To the west, the distal portions of the prograding clinoforms interfinger with the drift deposits of Site 1006. Site 1007, therefore, was the link between this basinal site and the proximal slope sites to the east. In addition, a higher percentage of microfossils with good preservation was expected here than in the more proximal Sites 1005, 1004, and 1003. Therefore, the main objectives of this site in regard to sea level were to (1) precisely date the sequence boundaries, (2) determine the facies in the distal portions of carbonate sequences, and (3) assemble a data set suitable to compare the sedimentary record with the oxygen isotopic record of the Neogene to recent sea-level fluctuations. Similarly as for the sea-level objectives, Site 1007 was also an intermediate site for the fluid-flow objectives. Interstitial-water chemistry and in situ temperature measurements should provide information about the fluid movement in the lower slope and, by comparison with the three previously drilled proximal sites, assess lateral changes in fluid chemistry. A logging suite, including a vertical seismic profile experiment, was performed for optimal correlation between the cores and the seismic data.

At Site 1007, the entire Neogene section and 20 m of Oligocene sediments were penetrated in a 1235.4 mbsf deep hole. Therefore, this site provides a complete sedimentary record of the Neogene sea-level changes. Its position at the base of the slope makes it the link between the proximal Sites 1003, 1004, and 1005 and the basinal Site 1006. Similar to site 1006, overall recovery was better than in the proximal sites and the planktonic foraminifers and nannofossils were more abundant and better preserved than in the proximal sites. As a result, a detailed biostratigraphy was established for the entire Neogene section. This enables the sequence boundaries at this site to be precisely dated and allows a comparison of the ages of the boundaries with the other sites. The comparison yields an excellent correlation between the sites, documenting the age consistency of the sequence boundaries and the chronostratigraphic significance of these seismic reflections. Furthermore, the biostratigraphic dating was of sufficient quality to record sedimentation rates within several individual seismic sequences, thus providing an independent record of the platform-derived sedimentation during sea-level highstands and the reduced pelagic sedimentation during sea-level lowstands. Sixteen seismic sequences were distinguished prior to drilling Site 1007. The good core recovery provides the facies information of these sequences. The facies succession indicates reduced or absent platform-derived sedimentation during the formation of the sequence boundaries, probably as a result of platform exposure during sea-level lowstands. Redeposited carbonates are present in the lower portion of the Miocene sequences. For example, turbidites and slump packages, in a more pelagic background sediment (lowstands), and biowackestones with more platform-derived material in the upper portions (highstands). With the transition into a steep-sided platform in the Pliocene, redeposited carbonates become more abundant in the upper parts of the sequences. This difference documents the relationship between platform morphology and highstand vs. lowstand shedding in carbonates. Facies and diagenesis act in concert to produce petrophysical differences within the sedimentary section. As a result, the logs reflect closely the sedimentary and stratigraphic record. All sequence boundaries can be clearly identified on the log data. A core-to-log-to-seismic correlation is possible by the time-depth conversion using the vertical seismic profile that was acquired in the open hole after logging.

In regard to the fluid-flow objectives, Site 1007 is also a link between the basinal and the proximal sites. As at all other sites, it shows evidence of a flushed zone in the upper 20 mbsf, which is somewhat shallower than in the proximal sites. The lower portion of the profile is dominated by diffusion, with local reactions involving the oxidation of organic material, the formation of pyrite, the precipitation and dissolution of carbonate minerals, and diagenesis of clay minerals and cherts controlling the concentration of various pore-water constituents.

In summary, with the completion of this deep site and a total depth (TD) within the Oligocene, Leg 166 provides a record of sea-level changes through the entire Neogene. The facies succession documents that the seismic sequences are indeed sea-level controlled. Furthermore, with the ability to precisely date the boundaries and several horizons within the sequences, the timing of these sea-level changes can be established. The well-preserved foraminifers at this site and Site 1006 will provide an oxygen isotopic record of the Neogene sea-level changes in the same transect. Interstitial-water geochemistry yields depth profiles that are indicative of stratiform fluid flow in the upper portions of the sections. Thus, a data set is collected that fulfills all the sea-level and fluid-flow objectives of the Leg 166 Bahamas Transect.

A nearly continuous section of Pleistocene to upper Oligocene sediments was recovered at Site 1007 at the toe-of-slope of present-day Great Bahama Bank. These deposits contain elements identified at more proximal Site 1003 and more distal Site 1006. This sedimentary succession is interpreted to record an interplay among: (1) change in platform-to-basin morphology; (2) sea-level variation; (3) pelagic input; and (4) ocean currents. In contrast to other sites drilled during Leg 166, the section at Site 1007 is characterized by an increased occurrence of turbidites and slumped intervals and by a relatively high amount of clay- and silt-sized siliciclastics in the late Pliocene and Pleistocene parts of the section. In addition, below 1120 mbsf sediments at Site 1007 are marked by the presence of compaction-dissolution features, namely anastomosing or wispy solution seams.

The Pleistocene section at Site 1007 is characterized by a meter-scale alternation between silt- and clay-rich sediment and silt- and clay-poor sediment. These alternations are similar to the clay cycles observed in the Pleistocene section at Site 1006, and are interpreted to reflect erosion of continent-derived siliciclastics during sea-level lowstands and incipient sea-level rise, and a subsequent increase in neritic and pelagic input following flooding. Seismic stratigraphy and biostratigraphic data indicate that the upper Pliocene section is thicker and characterized by a higher sedimentation rate relative to other sites. This thickness variation is caused by two processes: (1) an accumulation of mass-gravity flow deposits, which bypassed the upper slope and accumulated at Site 1007; and (2) an increase in the amount of current drift deposits. This latter increase could reflect a migration of the northward-flowing, Santaren Channel Current toward the platform during the late Pliocene and early Pleistocene.

As at other sites drilled on Leg 166, the sedimentary succession at Site 1007 records an important change in the mode of neritic carbonate production. At the base of Unit I (base of upper Pliocene), there is a sudden increase in the occurrence of platform-derived material, including aragonite needles and peloids. The turnover from skeletal- to aragonite needle-/peloid-dominated sediments probably reflects the coupled effects of climate change, and the transition of the Bahamas Bank from a carbonate ramp, characteristic of the Miocene, to the present-day, flat-topped carbonate platform.

The Miocene section at Site 1007 is nearly identical to the Miocene section recovered at Sites 1003, 1005, and 1006, and consists of alternating intervals of (1) well-cemented, decimeter- to meter-scale light-colored, clay-free intervals, which show no evidence of compaction; and (2) decimeter-scale dark-colored, relatively clay-rich intervals that show evidence of compaction. These alternations are interpreted to reflect changes in the rate of neritic carbonate input and the subsequent impact on the primary diagenetic potential of sediments. In this regard, light-colored, well-cemented intervals may reflect periods of higher neritic input (aragonite and high-Mg calcite) and the deposition of sediments with a higher diagenetic potential. In contrast, dark-colored, weakly cemented intervals may reflect periods of decreased neritic input and the deposition of sediments with higher amounts of low-Mg calcite.

Sediments at Site 1007 are divided into eight lithologic units on the basis of compositional and textural changes. Most unit boundaries correspond to (1) inferred periods of reduced sedimentation, (2) change in sediment composition, and (3) intervals of increased mass-gravity flow deposits.

Unit I (0-231 mbsf; Pleistocene to late Pliocene) consists of a succession of nannofossil ooze and variable lithified wackestones to packstones. Aragonite needles and peloids are an important but variable component in the silt- and fine sand-sized fraction. The disappearance of peloids marks the lower boundary of this unit. Unit I is subdivided into four subunits. Subunit IA (0-10.9 mbsf) is a sequence of nannofossil ooze, unlithified wackestone and packstone, which is interrupted by gravity-flow deposits. Subunit IB (10.9-43.5 mbsf) is characterized by meter-scale alternations between intervals of silt- and clay-rich sediments and intervals of silt- and clay-free sediments. The contact between Subunit IB and Subunit IC occurs at the top of the lowermost of two hardgrounds. Subunit IC (43.5-165 mbsf) encompasses a sequence of faintly laminated, unlithified peloidal wackestone to packstone. This succession is interrupted by an interval of partially lithified foraminifer wackestone and a slumped interval containing interbeds of unlithified packstone to floatstone. The contact between Subunit IC and ID is defined by a change in degree of lithification that coincides with a firmground. Subunit ID (165.8-203.1 mbsf) consists of slightly dolomitized wackestone and packstone.

Unit II (203.1-302.0 mbsf; early Pliocene) consists entirely of bioturbated light gray to pale yellow foraminifer nannofossil chalk. Foraminifers are the dominant allochem, whereas other bioclastic debris are minor constituents.

Unit III (302.0-362.6 mbsf; late Miocene) displays variable degrees of lithification of foraminifer wackestone, nannofossil chalk, and nannofossil limestone. In the upper part of the unit, a series of coarse-grained turbidites are intercalated. The boundary of the underlying Unit IV is placed above a series of fine-grained, laminated packstones.

Unit IV (362.6-696.4 mbsf; middle to upper Miocene) is made up of 5-10 cm thick layers of fine-grained packstone and an alternation between decimeter- to meter-scale intervals of densely cemented sediment with intervals of weakly cemented intervals that show evidence of compaction. These alternations probably reflect the rate of neritic input that is related to sea-level changes (see above).

Unit V (696.4-832.7 mbsf; middle Miocene) consists primarily of a succession of bioturbated foraminifer wackestone with minor intervals of packstone and mudstone. Turbidites are concentrated in the upper part of Unit V, whereas the lower part of the unit contains similar cyclic alternations of better and less cemented wackestones described above.

Unit VI (832.7-986.2 mbsf; early to middle Miocene) also contains bioturbated biowackestones with a small amount of packstones. In addition, several firmgrounds and thin clay-rich layers are observed within the unit.

Unit VII (986.2-1187.3 mbsf; early Miocene), like Units IV, V, and VI, is characterized by an alternation between well-cemented decimeter- to meter-scale intervals and decimeter-scale dark-colored intervals that show evidence of compaction. In addition, it also contains numerous calcareous turbidite deposits and clay-rich layers.

Unit VIII (1187.3-1235.4 mbsf; late Oligocene to early Miocene) consists of foraminifer wackestone and bioclastic wackestone arranged in alternations of decimeter- to meter-scale light and dark-colored intervals that are generally similar to those described in the overlying units. Black chert nodules and compaction/dissolution seams differentiate this unit from the overlying ones.

Sedimentation rates were determined on the basis of nannofossil and planktonic foraminiferal biostratigraphy. The average sedimentation rate for the Pleistocene interval is 5 cm/k.y. However, the top of Hole 1007B is older than 0.95 Ma. Obviously, current action along this part of the slope increased during the last 1 m.y. and caused non-deposition and/or erosion. A hiatus just below the Pliocene/Pleistocene boundary that lasted for approximately 0.4 m.y. might also be the result of current activity. The upper Pliocene interval is highly expanded with an average sedimentation rate of 21 cm/k.y. This is much higher than in time-equivalent intervals at the other transect sites, where sedimentation rates of about 2-3 cm/k.y. were found. The increased sedimentation rate is the combined result of deposition of platform-derived material that bypassed the upper slope and was deposited at the toe of the slope and the accumulation of drift sediments at Site 1007. The lower Pliocene package is bounded by a hiatus. The duration of the hiatus spanning the early/late Pliocene boundary is approximately 1 m.y. (3.2-4.2 Ma). The sedimentation rate below this hiatus is 17.5 cm/k.y. and is similar to the more proximal slope sites (Sites 1003, 1005) and in the Florida Straits (Site 1006). Below 304 mbsf, an interval of poor preservation, represents either an interval of very low sedimentation (<1 cm/k.y.) or contains a hiatus that straddles the Miocene/Pliocene boundary.

A late Miocene hiatus was detected at approximately 328 mbsf and spanned a period of approximately 2 m.y. Just above this unconformity, approximately 20 m of uppermost Miocene sediments were found. The sedimentation rate for this short section cannot accurately be determined, but it might be 1 cm/k.y. This may provide evidence for some platform production during the Messinian, or else it represents a lowstand wedge. The late Miocene is characterized by a high sedimentation rate (13 cm/k.y.). Sedimentation rates at the proximal Sites 1003 and 1005 were very similar, whereas Site 1006, located farther out in the basin, shows a much lower sedimentation rate (3 cm/k.y.; i.e., pelagic in nature). This sedimentation-rate pattern shows that the GBB was shedding material to the gently dipping slope during the late Miocene. Sedimentation rates in the middle and early Miocene can be divided into four cycles of alternating low (<2 cm/k.y.) and high (>5 cm/k.y) sedimentation. Slow sedimentation intervals occurred from 9.5 to 11.5 Ma, 13 to 15 Ma, 16.5 to 17.5 Ma, and 20.5 to 23 Ma and correlate to hiatuses of similar duration at Site 1003. Periods of faster deposition occurred from 11.5 to 13 Ma, 15 to 16.5 Ma, 17.5 to 20.5 Ma, and older than 23 Ma, corresponding to intervals at Site 1003 with similarly high sedimentation rates. These cycles represent increases and decreases in platform production in response to relative sea-level changes.

Geophysical and geochemical data acquired during logging of Hole 1007C provide detailed information on the sedimentary properties and structure of the strata. Log-to-core correlation permits significant interpretations about variations in sedimentation patterns on the toe-of-slope of GBB from the earliest early Miocene to Holocene. The general compatibility of the discrete data points from shipboard petrophysical measurements with the log data supports the integrity of the data sets. In general there is a downhole trend of increasing resistivity and sonic velocity. Small-scale and long-term excursions are superimposed over this general trend. These variations reflect the lithological and diagenetic variations in the core. Higher resistivity and velocity can be correlated approximately with sediments described as firmgrounds, hardgrounds, or turbidites. In addition, logs display little variation through monotonous sedimentary units. Furthermore, because the higher resistivity and velocity values in the log data coincide with sequence-stratigraphically important sedimentary units, they display all sequence boundaries precisely.

Sixteen seismic sequences were distinguished prior to drilling. Ages of the sequence boundaries were postulated from the biostratigraphic information of the adjacent sites. These predictions proved to be very accurate. In addition, the better preservation of the biostratigraphic markers at Site 1007 compared to the more proximal sites permit a refinement of some of the ages. For example, the early Pliocene sequence was not datable in the more proximal Sites 1003 and 1005 because of the absence of age diagnostic marker species. At this more distal site, a precise stratigraphy through this interval is possible and the basal sequence boundary is now dated as the top of the Messinian. For a comparison of the ages of the seismic reflection that mark the sequence boundaries, a vertical seismic profile was acquired for an accurate time-depth conversion. All the seismic sequence boundaries yield the same ages as in the adjacent sites. The age consistency of seismic reflections validates the basic assumption of sequence stratigraphy, which assumes that a chronostratigraphic significance to seismic reflections is correct. The good age control at this site and the entire transect allows for precise age dating of the sequence boundary and, thus, for the sea-level changes throughout the Neogene.

Three basic geochemical zones, which relate to zones observed previously, are present at Site 1007. First, there is an upper flushed zone wherein there are no changes in the conservative elements. There are only minimal changes in the non-conservative elements, such as Sr^{2+}, Ca^{2+}, and alkalinity. This zone is similar to that found at the upper slope sites (Sites 1003, 1004, and 1005), but differs in that minimal changes were observed in the concentration of Sr^{2+} at Site 1007. This contrasts with the slope sites, which exhibited no change in non-conservative parameters such as Sr^{2+} over this interval. Site 1007 is similar to the most distal site (Site 1006) in this regard. This flushed zone is also thinner than in the proximal sites, with a thickness of only 20 m compared to 40 m. Below the flushed zone, the concentration of the conservative elements, (Cl^- and Na^+) shows a diffusional relationship to the bottom of the hole. The concentration of K^+ decreases dramatically between 900 and 1000 mbsf related to diagenesis of clay minerals. In geochemical zone 2, concentrations of the non-conservative elements (Sr^{2+}, SO_4^{2-}, Ca^{2+}, NH_4^+, and alkalinity) show changes which are related to local reactions such as the degradation of organic material and the recrystallization of carbonate minerals. Immediately below the flushed zone, the SO_4^{2-} concentration decreases slightly as a result of the local oxidation of organic material. This gas is accompanied by an increase in the concentration of methane. The concentration of SO_4^{2-} again rises to seawater values at 400 mbsf and then decreases to zero below 600 mbsf. The removal of SO_4^{2-} marks the start of the third geochemical zone and corresponds to the appearance of concentrations of up to 10 ppm isobutane in the headspace samples. This is postulated to be of thermogenic origin. The concentration of Sr^{2+} in this interval is strongly controlled by the solubility of celestite. Once the SO_4^{2-} has been completely removed from the pore waters, the Sr^{2+} increases to over 5 mM at a depth of 950 mbsf. A maximum in the Ca^{2+} concentration between 350 and 400 mbsf indicates a probable zone of carbonate dissolution between 350 and 400 mbsf. Below this depth, Ca^{2+} concentrations decrease. When normalized to seawater Cl^- concentrations, this zone shows a net removal of Ca^{2+} from the pore waters.

Over the upper 900 mbsf the sediments consist of over 90% carbonate. Below this depth, concentration of carbonate decreases to between 60% and 80% with higher amounts of organic carbon (up to 1 wt%). Organic carbon is also higher in Unit IVB. The hole is dominated by LMC, although Unit I consists mainly of aragonite with small amounts of dolomite and HMC. Throughout the remainder of the hole, dolomite is a minor constituent with concentrations of up to 40% in small, isolated intervals. Quartz is a ubiquitous component throughout the core and there are documented occurrences of pyrite and clay minerals.

In summary, Site 1007 shows evidence of a flushed zone in the upper 20 mbsf, although profiles indicate that the flushing is slower than at the proximal sites and that it does not extend to as great a depth. The lower portion of the profile is dominated by diffusion, with local reactions involving the oxidation of organic material, the formation of pyrite, the precipitation and dissolution of carbonate minerals, and diagenesis of clay minerals and cherts controlling the concentration of various pore-water constituents.

Site 1007 completed the data set needed to address all the questions in regard to sea-level changes and fluid flow. A precise foraminifer and nannofossil biostratigraphy provides the age control on the depositional changes that are related to sea-level changes and the resulting sequence boundaries. This sedimentary record will add to the database that is needed to eventually establish the global synchrony of sea-level changes. Furthermore, the abundant, well-preserved foraminifers in the Bahamas Transect provide us with the unique opportunity to compare the sedimentary record with the oxygen isotopic proxy for sea-level changes. This comparison potentially will assess the causal relationship between the stratal pattern and sea-level changes.

The geochemical profiles at Site 1007 indicate, as in the other sites, that there is active fluid flow in the upper portion of the strata. The occurrence of the change of gradients at similar depth along the transect provides strong evidence that flow is at least partially horizontal and related to stratigraphic boundaries. With increasing depth, diffusive processes become the dominant transport mechanism.

Sites 1008/1009

The primary objective of Sites 1008/1009 was to obtain heat flow and interstitial-water geochemistry measurements from a second area of the margin of Great Bahama Bank to compare with data from Sites 1003-1007. This approach was necessary to help support our findings regarding fluid flow and diagenetic reactions in the margin of the platform. A secondary objective was to retrieve a high-resolution section of Holocene sediment for the study of recent climate change.

Sites 1008 and 1009 penetrated thick Pleistocene sections. At Site 1008, the age at the base of the hole (134.5 mbsf) is 1.44 Ma, with sedimentation rates varying between 4.5 and 16 cm/k.y. At Site 1009 a similar age was attained at a depth of 226.1 mbsf, with sedimentation rates between 5 and 55 cm/k.y. Eight seismic sequences can be recognized in the drilled section that are separated from each other by seven seismic boundaries. The strata at Sites 1008 and 1009 consist of lithified to partially lithified peloidal and bioclastic mudstones, wackestones, packstones, and grainstones with interbedded foraminifer nannofossil ooze. Most of the SSBs correlate with distinct layers in the cores, that are dark in color, coarse grained, and show signs of submarine cementation. Adara and WSTP temperature measurements revealed an irregular heat flux in the upper 40 mbsf and a much lower heat flux (20 mW vs. 40 mW) in the lower portion of the profile, as compared to Sites 1003-1007. Pore-water geochemistry profiles showed little variation in the upper 30 mbsf. Below this zone sulfate reduction and other diagenetic reactions were prevalent.

Two major lithologic units were distinguished at both Sites 1008 and 1009.

Unit I (0-78.2 mbsf, Site 1008; 0-147.15 mbsf, Site 1009) is latest Pleistocene to Holocene in age. Subunit IA (0-27.1 mbsf, Site 1008; 0-22.02 mbsf, Site 1009) consists of a coarsening-upward, pale-yellow to white, unlithified, peloidal wackestone grading into wackestone and mudstone, with minor to moderate bioturbation. The base of this subunit is marked in both sites by a bored and encrusted hardground. Subunit IB (27.1-78.2 mbsf, Site 1008, 22.02-98.71 mbsf, Site 1009) consists of multiple coarsening-upward sequences separated by harder layers. The sequences are composed of unlithified peloidal mudstones at the base and peloidal packstones at the top, which also correspond to cycles in physical properties. Characteristically they have relatively low velocities, densities, and gamma-ray values at their base that increase toward the top. The floatstones contain large gray lithoclasts composed of pteropod and planktonic foraminifer wackestone to packstone. The clasts are cemented and bored and are interpreted as being the remnant of a marine hardground. Subunit IC (98.71-147.15, Site 1009) was not recognized at Site 1008. It contains four coarsening-upward intervals and is separated from Unit IB by a fragmented hard layer consisting of pteropod biopackstone. Subunit IA at Site 1008 has a sedimentation rate of 4.5 cm/k.y., whereas subunit IB has a rate of 16 cm/k.y. At Site 1009, the sedimentation rates are 18 cm/k.y. throughout Subunit IA, up to 35 cm/k.y. in Subunit IB and 7 cm/k.y. in Subunit IC.

Unit II (78.2-134.5, Site 1008; 147.15-226.1, Site 1009) consists of unlithified lithoclastic and bioclastic floatstone. At Site 1009 two hardgrounds are recognized in this sequence. At Site 1008, the sedimentation rate in Unit II is 8 cm/k.y. At Site 1009 sedimentation rates are between 22 and 55 cm/k.y. throughout Unit II.

At both sites a number of alternations in sediment composition, color, and mineralogy can be recognized, which probably correspond to sea-level changes. Lowstands are characterized by higher concentrations of low-Mg calcite that have a darker color compared to highstands which contain abundant aragonite and high-Mg calcite. Dolomite becomes a minor component of the sediment below 60 mbsf in Site 1008 and 120 mbsf at Site 1009, and percent carbonate was generally higher than 95% throughout.

Sites 1008 and 1009 recovered extremely expanded sections of Pleistocene and Holocene sediments. The nannofossil biostratigraphy indicates the presence of zones NN19 to NN21. The planktonic foraminifer record is restricted to N22. Sediments were substantially reworked in the lower part of the record.

The youngest seismic sequence s appears at Site 1009 at 29 mbsf and at Site 1008 at 9.6 mbsf. The age of the SSB (0.15-0.12 Ma) probably corresponds to the last sea-level lowstand at the Pleistocene/Holocene boundary. SSB T corresponds to 48 mbsf at Site 1009 and 14.5 at Site 1008 and has an age of 0.20 to 0.25 Ma. These two boundaries, as well as SSB U, appear in both holes slightly deeper than high-velocity layers, allowing for the possibility that too high a velocity was assumed for these sediments in the depth/time conversions. Sequence w has its lower boundary at 126 and 53.2 mbsf at Sites 1009 and 1008, respectively. The associated age of SSB W which might correlate to a high-velocity layer 13 m higher in the core, is 0.7-0.062 Ma. The rest of the holes show two prominent velocity deviations coinciding with SSBs X and Y.

Based on the pore-water geochemistry, two distinct geochemical zones were identified within Sites 1008 and 1009. An upper zone, extending from the seafloor to 40 mbsf, is characterized by an absence of significant changes in the interstitial pore-water geochemistry. This flushed zone is similar to those observed at Sites 1006 and 1007, in that there was slight evidence of carbonate recrystallization reactions in the form of a small, but nevertheless significant, increase in the Sr concentration. Sites 1003, 1004, and 1005 showed no evidence of such an increase. The upper zone gradually merges into a region with elevated chlorinity, up to 730 mM at Site 1009 and 670 mM at Site 1008. This zone shows a small reduction in sulfate and large increases (up to 1600 μM) in Sr. Calcium and Mg are reduced relative to their seawater values in this interval, indicating carbonate mineral precipitation. Methane and hydrogen sulfide reached concentrations of 100 and 10,000 ppm, respectively, within the zone of low sulfate.

Heat flow at both sites is significantly lower than at Sites 1003-1007. At Sites 1008 and 1009 the geothermal gradient is approximately 27°C/km and 17°C/km respectively. This compares to approximately 35°C/km for the northern sites. The low heat flow may indicate regional cooling as a result of the inflow of bottom seawater, perhaps deeper in the sedimentary section.

CONCLUSIONS

The primary objective of Leg 166 was to address fundamental questions regarding sea level. To attain this objective, five sites in the Straits of Florida were drilled during Leg 166, completing a transect through prograding carbonate sequences formed in response to sea-level fluctuations along the western margin of the Great Bahama Bank. Two boreholes drilled previously on the western Great Bahama Bank as part of the Bahamas Drilling Project represented the shallow-water sites of the transect. The primary goal of the transect was to document the platform-margin record of the Neogene–Holocene sea-level changes by determining the ages of the major unconformities and comparing the timing of these unconformities with ages predicted from the oxygen isotopic record of glacio-eustasy. Core borings along the complete transect document the facies variations associated with oscillations of sea level and, thus, the sedimentary response of the carbonate environment to sea-level changes. The correlation between the two independent records of sea-level changes, sequence stratigraphy and oxygen isotope proxy, has the potential to evaluate rate and amplitude of eustatic vs. relative sea-level changes and to establish a causal link between glacioeustasy and the stratigraphic pattern.

Primary Leg Objectives

The main objective of the proposed drilling transect along the western margin of the Great Bahama Bank was to study the record of Neogene–Quaternary sea-level fluctuations in the prograding sequences. Within this sea-level objective were the following goals:

1. Determine the timing of the sequence boundaries and relative sea-level fluctuations to acquire the necessary database for the possible global synchroneity of these fluctuations.

   Conclusions: Calcareous nannofossils and planktonic foraminiferal biostratigraphic datums were used to establish an age-depth relationship for each of the sites drilled as part of the Bahamas Transect (Sites 1003-1007) on the leeward slope of GBB. Many biohorizons from both groups were identified, establishing a framework for intersite correlation, which was transferred into time using the Geomagnetic Polarity Time Scale of Berggren et al. (1995). The latter step was the most important to obtain absolute ages to fulfill one of the objectives of this leg; testing the age consistency of the sequence boundaries observed in the seismic records and logging data in combination with lithological changes observed in the recovered sedimentary section. The overall consistency in the relative position of planktonic foraminiferal and nannofossil datums means that a reliable framework for intersite correlation was established for the Bahamas Transect sites.

   Sequence analysis was performed on the seismic data prior to drilling. The reflections identified as sequence boundaries were traced to the slope and basinal areas of the Leg 166 Bahamas Transect sites. By reaching the Oligocene at Site 1007, a complete record for the sequence stratigraphic architecture is available for the entire Neogene. We identified 17 sequences in the Neogene section. At the Leg 166 sites, most of the sequence boundaries are conformable; however, truncation is observed in the more proximal sites.

   The time/depth conversion obtained from vertical seismic profile experiments allowed us to correlate the sequence boundaries to the cores. All sequence boundaries coincide, within seismic resolution of about 10 m, with a facies change indicative of a sea-level change. The exact position of the boundaries is recorded on the log data, which has a better resolution than the seismic data. The age at the correlative depth was calculated using biostratigraphic datums and extrapolating sedimentation rates between datums. Although this procedure carries the uncertainty of both the exact position of the biostratigraphic datums and the seismic resolution, the sequence boundaries showed consistent ages along the seismic reflections. This result is exciting as it confirms one of the major assumptions of sequence stratigraphy that seismic reflections are time lines.

The ages of the sea-level changes in the Neogene were estimated from the ages of the sequence boundaries. In the proximal sites, where several of the sequence boundaries are associated with erosion that occasionally is detected by a hiatus, the age of the boundary was taken from the distal, conformable locations. In light of the resolution problem, the ages of the sequence boundaries probably have an error bar of approximately 0.2 m.y. Nevertheless, the ages indicate that the seismic sequences along the Bahamas Transect record most of the known major (third-order) sea-level changes in the Neogene. Shore-based log-seismic correlation and detailed biostratigraphic analysis will refine the age model for these sea-level changes.

2. Determine the stratigraphic response of carbonates to sea-level changes of variable frequency by analyzing the facies of the stacked depositional sequences. Special emphasis was placed on documenting the amount and nature of lowstand deposits in carbonates and the hierarchical stacking of high-frequency cycles into seismic sequences.

   Conclusions: Overall core recovery was sufficient (55.3%) to document the facies successions throughout the cores. The facies successions contain indications of sea-level changes on two different scales. First, there are high-frequency alternations of layers containing more platform-derived material with layers consisting of more pelagic sediments. In the Pleistocene and Pliocene periplatform section, these alternations are reflected in the ratio between neritic components and nannofossils and mineralogically between aragonite and low Mg-calcite. In previous studies these cycles have been shown to correlate to the orbitally forced, high-frequency, sea-level changes in the Quaternary. We found similar decimeter- to meter-scale, high-frequency changes in facies in the Miocene sections in all the holes. The Miocene cycles display a decimeter-thick alternation of light-colored, bioturbated, well-cemented biowackestones and less cemented, darker biowackestones with compacted burrows. The Miocene alternations are interpreted to reflect changes in the rate of neritic input (metastable aragonite and high-Mg calcite). Thus, the well-cemented wackestones represent higher neritic input and have a greater diagenetic input than the less-cemented intervals with less neritic input. Because of the color changes and the cementation differences, these cycles are also recorded in the color reflectance and the logs. Formation MicroScanner data provided a continuous record of these cycles at two sites, which will be analyzed to determine the frequency of these cycles in the Miocene.

A repetitive pattern of facies succession on the order of tens to hundreds of meters thick, documents a sedimentary record of longer-term sea-level changes. These larger-scale patterns are imaged in the seismic sequences. Similarly, as in the small-scale cycles, changes in the amount of platform-derived material indicate periods of high and low sea level. Platform exposure during low sea level is reflected in reduced sedimentation rates, occasionally leading to hardground formation on the slope. In addition, erosion of the platform margin during these periods is documented by the deposition of coarse-grained packstones and floatstones in pelagic-rich background sediments. Erosional truncation is also observed in the proximal slope sites, which leads to hiatuses in the biostratigraphic successions. Cycles are best developed during sea-level rises and usually compose the middle part of the sequences. Redeposition of platform carbonates occurs again in the upper portion of the sequences. This pattern is best developed in the Miocene when the platform had a ramp-like morphology. In the Pliocene and Pleistocene, the bulk of the sediments, especially in the more proximal locations, are dominated by thick successions of fine-grained material, but turbidites occur preferentially in the upper portions of the sequences. More mass-gravity flow deposits are found in the distal sites, indicating that the steep upper slopes are bypassed by these flows.

3. Retrieve the low-latitude isotopic signals of the Ice House World in the Neogene and Quaternary and compare it with the stratigraphic record, potentially to document a causal link between eustasy and sequence stratigraphic pattern.

   Conclusions: To compare the sedimentary record of the sea-level changes with the oxygen isotopic proxy, a basinal hole (Site 1006) was drilled. The core far exceeded expectations as most conventional nannofossil and planktonic foraminifers were found in the middle Miocene to Pleistocene section. In addition, recovery was very high and the preservation of the foraminifers was good throughout the recovered section. Thus, all the prerequisites are in hand in the same transect to establish an oxygen isotopic record of the sea-level changes. The correlation of the sedimentary and the isotopic record will enable us to assess the causal relationship between sea-level changes and the sequence stratigraphic pattern, thereby fulfilling the third objective within the sea-level theme.

4. Estimate the magnitude and rate of sea-level changes using age and recovered facies for a precise subsidence analysis.

   Conclusions: Estimating the rate and magnitude of sea-level changes will require shore-based analyses including further refinement of the age model (detailed biostratigraphic analysis and paleomagnetic, O- and Sr-isotopic analyses) and detailed facies analyses of core samples and logs and log-seismic correlation .

5. Objective: To assess the processes responsible for fluid circulation in platforms by sampling slope sediments and analyzing their pore-water chemistry.

   Conclusions: One of the primary objectives of Leg 166 was to investigate the possibility of fluid-flow processes through the margin of Great Bahama Bank. The association of the fluid chemistry and heat-flow sampling program with the sea-level objectives means that changes in fluid chemistry can be examined not only as a function of age and depth, but also within a sequence stratigraphic framework. This approach is therefore fundamentally different from other investigations of pore-water profiles along carbonate platforms, which in most instances only drilled single holes.

   The clearest evidence for active recharge of fluids through the margin of GBB is derived from the nonsteady-state pore-water profiles of both conservative and nonconservative elements in the upper 100 mbsf obtained from both the northern (Sites 1003-1007) and southern transect (Sites 1008-1009). A zone, confined to the upper 40 mbsf, was identified (the flushed zone) in which there is an absence of geochemical gradients in both conservative and nonconservative constituents. The geochemical data in this interval shows essentially no change from bottom seawater concentrations for all of the normally measured cations and anions. Sites 1006 and 1007, which are situated farther from the platform, also have a flushed zone, but it is reduced in thickness and exhibits small, but nevertheless significant, increases in Sr^{2+}. The majority of these sites also showed irregular temperature profiles in this portion of the sedimentary column. A similar finding of an upper flushed zone approximately 40 m thick is also seen at the sites drilled along the more southerly transect. We propose that the absence of geochemical gradients and the irregular temperature profiles support the notion that there is advection of seawater through this portion of the sedimentary column. The presence of small increases in Sr^{2+} at the more distal sites indicates that fluid flow here is reduced relative to the platform. Below the flushed zone, there is a sharp change in the concentrations of both conservative and nonconservative elements. The SO_4^{2-} concentration decreases sharply, while alkalinity and Sr^{2+} increase. The nature of these gradients are not steady state and reflect depression by a downward advecting fluid. An unexpected finding at all the sites drilled was the increase in Cl^- concentration with increasing depth. This increase is probably a result of the diffusion of Cl^- and Na^+ from an underlying brine or evaporite deposits.

Based on the evidence from the seven sites drilled during Leg 166, there is clear evidence that a mechanism exists which produces active exchange between the upper 40 m of sediments and the bottom waters. At the present time we do not know the precise mechanism involved in the flushing mechanism, only that it exists. The observations are, however, consistent with water being drawn into the platform by the mechanism known as Kohout convection. In this mechanism the temperature difference between the platform interior and the adjacent seaways causes underpressure to develop within the platform, drawing water through the flanks of the platform.

Secondary Leg Objectives

A third objective of Leg 166 was to assess the paleoceanographic changes in the Straits of Florida. Several major changes have occurred in the Earth's climate, fauna, and ocean circulation from the mid-Cretaceous to the present. The sediments in the seaways of the Bahamian archipelago potentially record most of these events, many of which are important global problems. For example: the onset and variations in the Florida Current, the record of the Paleogene "Doubthouse" Earth and transition to the Neogene "Icehouse," the influence of the Cuban collision, the K/T boundary, and the mid-Cretaceous drowning of the megabank.

Conclusions: Although lack of time precluded recovery of extensive Paleogene and older sediments, an excellent Neogene sedimentary section was recovered that will allow many of the paleoceanographic objectives to be pursued in post-cruise studies. In particular, the sedimentary section at Site 1006 consists of mixed pelagic and bank-derived carbonates with varying amounts of clay material, believed to have been derived from Cuba and Hispaniola. The excellent continuous sedimentary sequence recovered contains abundant well-preserved foraminifers. Furthermore, the abundant pelagic biogenic components are less diluted by platform-derived material and microfossil preservation is less affected by diagenesis than in the upper slope sites (Sites 1003, 1004, and 1007). The expanded Pliocene and upper Miocene sequences, combined with the excellent preservation, will make this a classic site for upper Neogene paleoceanography in the low-latitude Atlantic. In addition, changes in the sediment composition are postulated to fluctuate in conjunction with variations in the strength of the Florida Current. We should be able to correlate these variations with changes in sea level as recorded by the prograding and regressive sequences at platform sites and the oxygen isotopic signature of the foraminifers.

REFERENCES

Berggren, W.A., Kent, D.V., Swisher, C.C., III, and Aubry, M.P., 1995. A revised Cenozoic geochronology and chronostratigraphy. *In* Berggren, W.A., Kent, D.V., and Hardenbol, J. (Eds.), Geochronology, Time Scales and Global Stratigraphic Correlations: A Unified Temporal Framework for an Historical Geology, *Soc. Econ. Paleont. Min. Special Volume*, 54:129-212.

Berggren, W.A., Kent, D.V., and Van Couvering, J.A., 1985. The Neogene: Part 2. Neogene geochronology and chronostratigraphy. *In* Snelling, N.J. (Ed.), *The Chronology of the Geological Record.* Geol. Soc. London Mem., 10:211-260.

Chaisson, W.P., and Pearson, P.N., in press. Planktonic foraminifer biostratigraphy at ODP Site 925, western tropical Atlantic: the last 12 m.y. *In* Curry, W.B., Shackleton, N.J., Richter, C., et al. *Proc. ODP, Sci. Results*, 154: College Station, TX (Ocean Drilling Program).

COSOD-II, 1987. Report of the Second Conference on Scientific Ocean Drilling: Strasbourg (Joint Oceanographic Institutions, Inc.).

Davies, P.J., McKenzie, J.A., Palmer-Julson, A., et al., 1991. *Proc. ODP, Init. Repts.*, 133: College Station, TX. (Ocean Drilling Program).

Elderfield, H., Swart, P.K., McKenzie, J.A., and Williams, A., 1993. The strontium isotopic composition of pore waters from Leg 133: N.E. Australian margin. *In*: Davies, P.A., McKenzie, J., and Palmer-Julson, A., (Eds.), *Proc. ODP, Sci. Results*, 133: College Station, TX (Ocean Drilling Program), 473-480.

Joint Oceanographic Institutions, Inc., Long Range Plan, 1996. *Ocean Drilling Program Long Range Plan, Understanding our Dynamic Earth Through Ocean Drilling*. Joint Oceanographic Institutions, Inc.

Joint Oceanographic Institutions, Inc., Long Range Plan, 1990. *Ocean Drilling Program Long Range Plan, 1989–2002*. Joint Oceanographic Institutions, Inc.

Kastner, M., and Brass, G., 1990. USSAC-JOI Workshop on fluid flow, Lake Arrowhead.

Kohout, F.A., 1967. Ground-water flow and the geothermal regime of the Floridian Plateau. *Transactions-Gulf Coast Geol. Soc.*, 17:339-354.

Miller, K.G., Wright, J.D., van Fossen, M.C., and Kent, D.V., 1994. Miocene stable isotopic stratigraphy and magnetostratigraphy of Buff Bay Jamaica. *GSA Bulletin*, 106:1605-1620.

Paull, C.K., Fullager, P.D., Bralower, T.J., and Rohl, U., 1995. Seawater ventilation of mid-Pacific guyots (Sites 865 to 868). *In* Winterer, E.L., Sager, W.W., Firth, J.V., and Sinton, J.M., (Eds.), *Proc. ODP, Sci. Results*, 143: College Station, TX (Ocean Drilling Program), 231-244.

Sato, T., Kameo, K., and Takayama, T., 1991. Coccolith biostratigraphy of the Arabian Sea. *In* Prell, W.L., Niitsuma, N., et al., 1991. *Proc. ODP, Sci. Results*, 117: College Station, TX (Ocean Drilling Program), 37-54.

Swart, P.K., Elderfield, H., and Beets, K., in press a. The $^{87}Sr/^{86}Sr$ ratios of carbonates, phosphorites, and fluids collected during the Bahama Drilling Project cores Clino and Unda: Implications for dating and diagenesis. *In*: R.N. Ginsburg (Ed.), *The Bahamas Drilling Project*. SEPM (Contr. to Sed.).

Swart, P.K., Elderfield, H., and Ostlund, G., in press b. The geochemistry of pore fluids from bore holes in the Great Bahama Bank. *In* R.N. Ginsburg (Ed.), *The Bahamas Drilling Project*. SEPM (Contr. to Sed.).

Watkins, J.S., and Mountain, G. S., 1990. Role of ODP in the investigation of global changes in sea-level. *JOI/USSAC Workshop El Paso, 1988*.

Zhang, J., Miller, K.G., and Berggren, W.B., 1993. Neogene planktonic foraminiferal biostratigraphy of northeastern Gulf of Mexico. *Micropaleontology*, 39:299-326.

FIGURE CAPTIONS

Figure 1. Location map of the Bahamas showing Leg 166 site-survey lines. Sites 1003 through 1007 are located in area A. Sites 1008 and 1009 are located in area B.

Figure 2. Cross section through the Great Bahama Bank displaying the complicated internal architecture of the bank. Two nuclear banks, Andros and Bimini, coalesced by the infilling of an intraplatform seaway, the Straits of Andros. Progradation of the western margin of the platform during the Neogene expanded the bank more than 25 km into the Straits of Florida (from Eberli et al., 1994).

Figure 3. Lithostratigraphic summary of Leg 166 Bahamas Transect (Sites 1008 and 1009 drilled ~100 km to the south are not shown).

Figure 4. Age-correlation diagram of the Leg 166 Bahamas Transect (Sites 1008 and 1009 drilled ~100 km to the south are not shown).

Figure 5. Summary sedimentation rate diagram for Leg 166 sites. Data were obtained from calcareous nannofossils and planktonic foraminifers.

Figure 6. Seismic line showing the prograding sequences at the western margin of the GBB with the locations of the Bahamas Transects drilled during Leg 166. Sequence boundaries were labeled A-I, K-R. A SSB between P and Q was recognized during the cruise and was labeled P2. SSB R was not peneterated during Leg 166.

Figure 7. Same seismic line as Figure 6 with ages of sequence boundaries calculated using biostratigraphic datums and extrapolating sedimentation rates between datums. Despite the uncertainty of both the exact position of the biostratigraphic datums and the seismic resolution, the sequence boundaries show consistent ages along the seismic reflections.

Figure 8. Interstitial water profiles from Leg 166 sites illustrating downhole changes in Cl^-.

Figure 9. Interstitial water profiles from Leg 166 sites illustrating downhole changes in Sr^{2+}.

Figure 10. Contour map of the pore-water Cl^- concentrations along the Leg 166 sites of the Bahamas Transect.

Table 1. Calcareous nannofossils and planktonic foraminiferal biostratigraphic datums.

Event	**Nanno-fossil Age (Ma)**	**Foraminifer Age (Ma)**	**Site 1006 Depth (mbsf)**	**Site 1007 Depth (mbsf)**	**Site 1003 Depth (mbsf)**	**Site 1004 Depth (mbsf)**	**Site 1005 Depth (mbsf)**
B *E. huxleyi*	0.25		4.24		14.14	19.43	20.49
T *P.lacunosa*	0.41		20.53		57.23	38.56	69.6
T *R.asanoi*	0.85		39.53		86.46	81.16	126.56
T *Gephyrocapsa* spp. (lg)	1.2		48.49	14.23	96.98		172.74
B *Gephyrocapsa* spp. (lg)	1.44		68.03	31.67			182.88
B *G.caribbeanica*	1.72		91.78	43.54	113.19	152.03	190.49
B *Gr.truncatulinoides*		2	97.69	53.54	123.75		
T *Gr.limbata*		2.4	116.8	53.54	132.70	186.41	
T *D.altispira*		3.1	145.22	200.34	142.90		226.72
T *R.pseudoumbilica*	3.6		172.53	200.34	155.79		247.52
T *G.nepenthes*		4.2	240.275	200.34	197.98		274.1
B *Ceratolithus rugosus*	4.7		325.98	287.61			365
T *D.quinqueramus*	5.6		383.415				
T *Reticulofenestra* spp(sm)	*6.5*		*417.8*	*304.30*			*415.98*
B *Gs.conglobatus*		6.8	436.04	327.87	355.65		415.98
B *Gr.cibaoensis*		7.7	483.07	327.87	355.65		415.98
B *Gs.extremus*		8.1	492.045	327.87	355.65		415.98
T *D.neohamtus*	8.7		500.95	327.99	355.65		415.98
T *D.hamatus*	9.4		530.48	432.99	461.46		415.98
B *D.hamatus*	10.7		567.445	481.68	531.60		495.28
B *C.coalitus*	11.3		602.51	503.69	555.10		582.355
T *Gr.mayeri*		11.4	595.385	481.69	561.04		595.78
B *G.nepenthes*		11.8	625.075	532.75	630.52		595.78
T *Fohsella* spp		11.9	639.96	542.48	641.30		670.895
B *Gr.fohsifohsi*		12.7	682.015	769.40	802.55		
T *C.floridanus*	13.2		696.27	742.12	780.00		
T *S.heteromorphus*	13.6			780.59	856.84		
B *Gr.praefoshi*		14		791.54	910.76		

Event	Nanno-fossil Age (Ma)	Foraminifer Age (Ma)	Site 1006 Depth (mbsf)	Site 1007 Depth (mbsf)	Site 1003 Depth (mbsf)	Site 1004 Depth (mbsf)	Site 1005 Depth (mbsf)
T *P. sicana*		14.8		800.20	910.76		
B *O.universa*		15.1		808.36	910.76		
T *H.altiaperta*	15.6			857.50	1058.06		
B *P.sicana*		16.4		915.05	1089.72		
T *C.dissimilis*		17.3		925.35	1089.72		
T *S.belemnos*	18.3			967.44	1108.08		
B *Ge.insueta*		18.8		973.41	1140.00		
B *S.belemnos*	19.2			1003.04	1171.86		
B *Gs.altiapertura*		20.5		1086.75	1204.13		
T *Gr.kugleri*		21.5		1099.62	1204.13		
B *D.druggi*	23.2			1117.85	1242.52		

Table 2. Ages of seismic sequence boundaries (SSB).

SSB	Site 1005 (Ma)	Site 1004 (Ma)	Site 1003 (Ma)	Site 1007 (Ma)	Site 1006 (Ma)	Composite Age (Ma)	Series/ Epoch	Stage
A	0.1	0.16	0.09			0.1	Holo./Pleist.	Holo./Pleist.
B	0.6	0.73	0.25			0.6	Pleistocene	Pleistocene
C	1.3	1.7	1.2-1.6	1.5-1.7	1.8	1.7	Pleist./Plio.	earliest Pleist.
D	2.9	2.6	3.1	3.2-4.2	3.1	3.1	late/early Plio.	late Pliocene
E	3.6		3.8	3.2-4.2	3.6	3.6	late early Plio.	early/late Plio.
F	6		5.6	5.5-6.4	5.55	5.6	late Miocene	Messinian
G	6.2-8.8		6.2-8.7	8.7	8.7	8.7	late Miocene	Tortonian
H	9.4		9	9.4	9.4	9.4	late Miocene	Tortonian
I	11.3		10.1	10.9-11.4	10.7	10.7	late/mid. Mio.	Tortonian
K			12.2	12.1	12.4	12.1	middle Miocene	Seravallian
L			12.7	12.5	12.7	12.7	middle Miocene	Seravallian
M			13.6-15.1	15.1		15.1	middle Miocene	Langhian
N			16	16.2-16.4		16	middle Miocene	Langhian
O			18.4	18.2		18.3	early Miocene	Burdigalian
P			19.2	19.4		19.4	early Miocene	Burdigalian
P2			19.8-23.2	23.2		23.2	early Miocene	Aquitanian
Q				23.7		23.7	early Miocene	Aquitanian
							Oligocene	Chattian

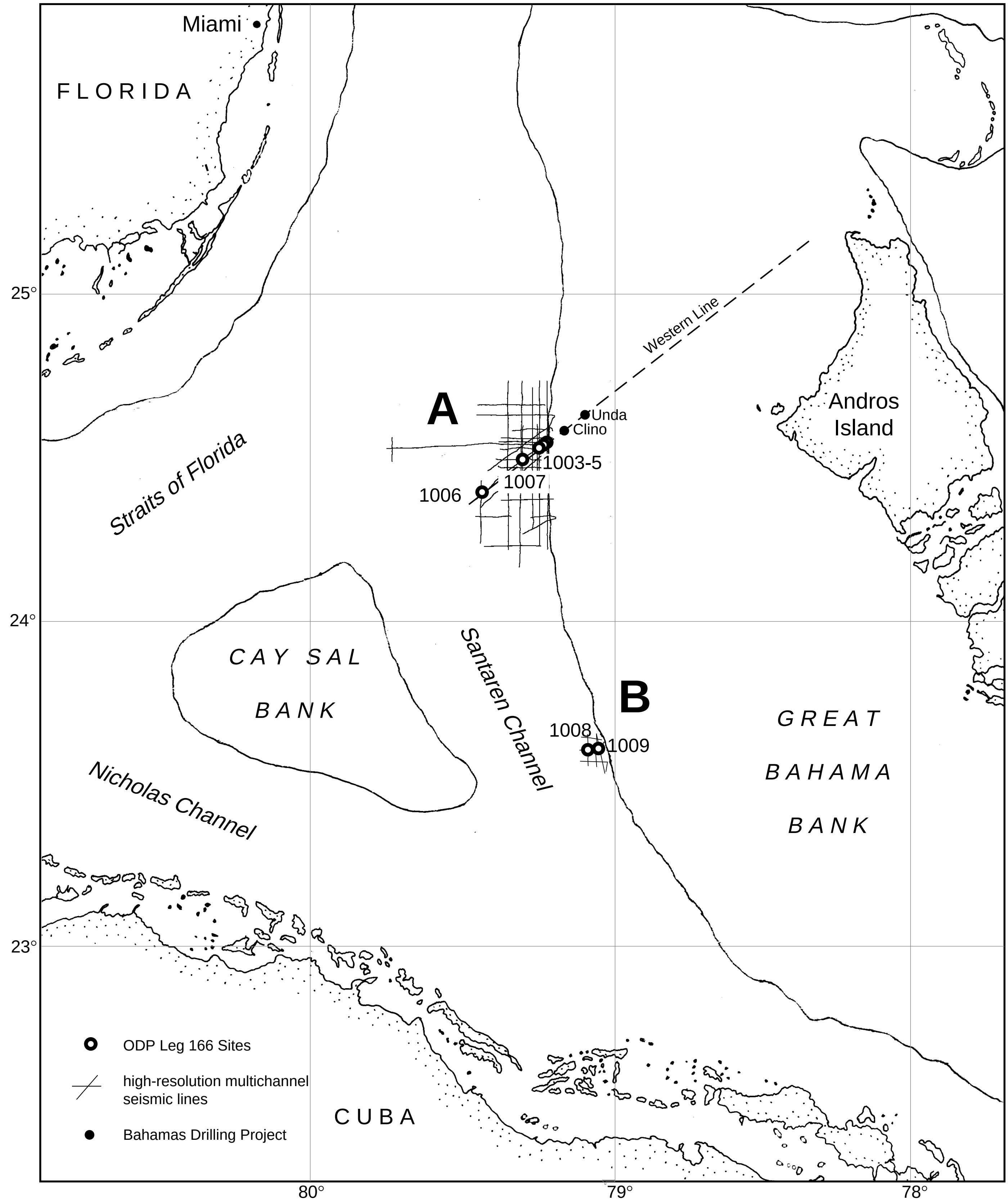
Miami
FLORIDA
25°
24°
23°
80°
79°
78°
Western Line
A
Unda
Clino
1003-5
1007
1006
Straits of Florida
Andros
Island
CAY SAL
BANK
Santaren Channel
B
1008
1009
GREAT
BAHAMA
BANK
Nicholas Channel
ODP Leg 166 Sites
high-resolution multichannel seismic lines
Bahamas Drilling Project
CUBA

Figure 1

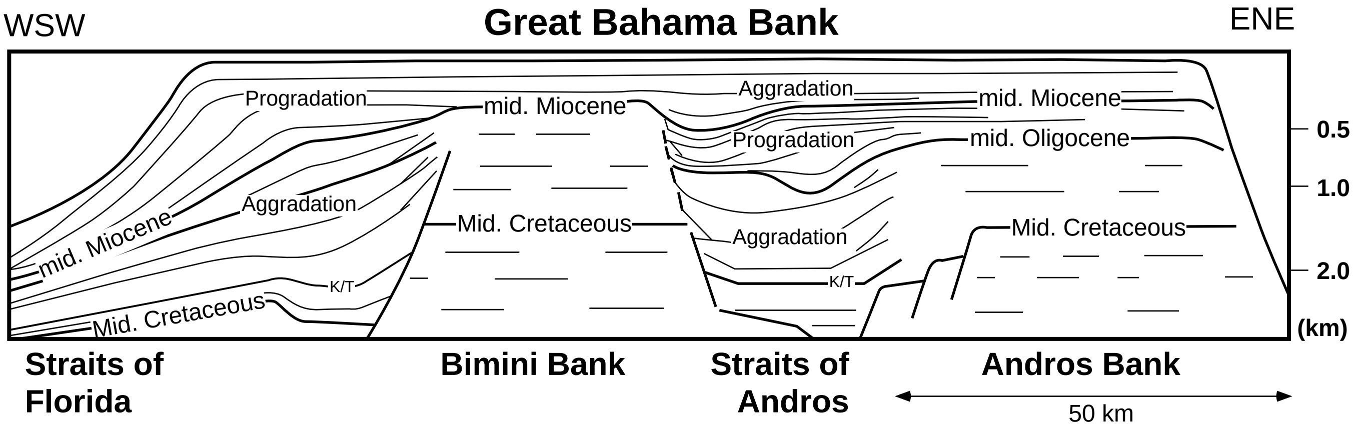
WSW
Great Bahama Bank
ENE
Progradation
mid. Miocene
Aggradation
mid. Miocene
Progradation
mid. Oligocene
mid. Miocene
Aggradation
Mid. Cretaceous
Aggradation
Mid. Cretaceous
K/T
K/T
Mid. Cretaceous
0.5
1.0
2.0
(km)
Straits of Florida
Bimini Bank
Straits of Andros
Andros Bank
50 km

Figure 2

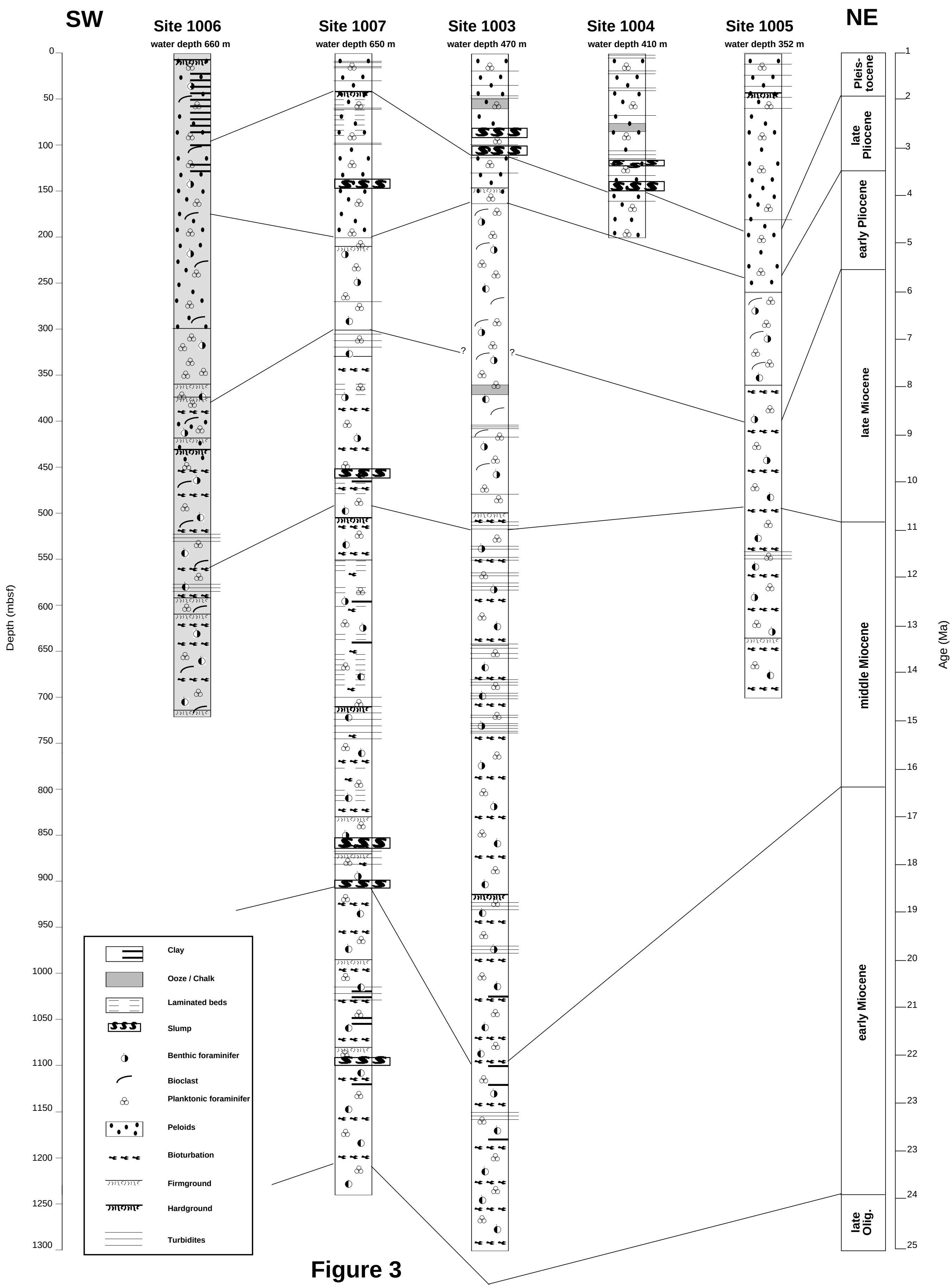
SW
Site 1006
water depth 660 m
Site 1007
water depth 650 m
Site 1003
water depth 470 m
Site 1004
water depth 410 m
Site 1005
water depth 352 m
NE
Depth (mbsf)
Age (Ma)
Pleis-tocene
late Pliocene
early Pliocene
late Miocene
middle Miocene
early Miocene
late Olig.
Clay
Ooze / Chalk
Laminated beds
Slump
Benthic foraminifer
Bioclast
Planktonic foraminifer
Peloids
Bioturbation
Firmground
Hardground
Turbidites

Figure 3

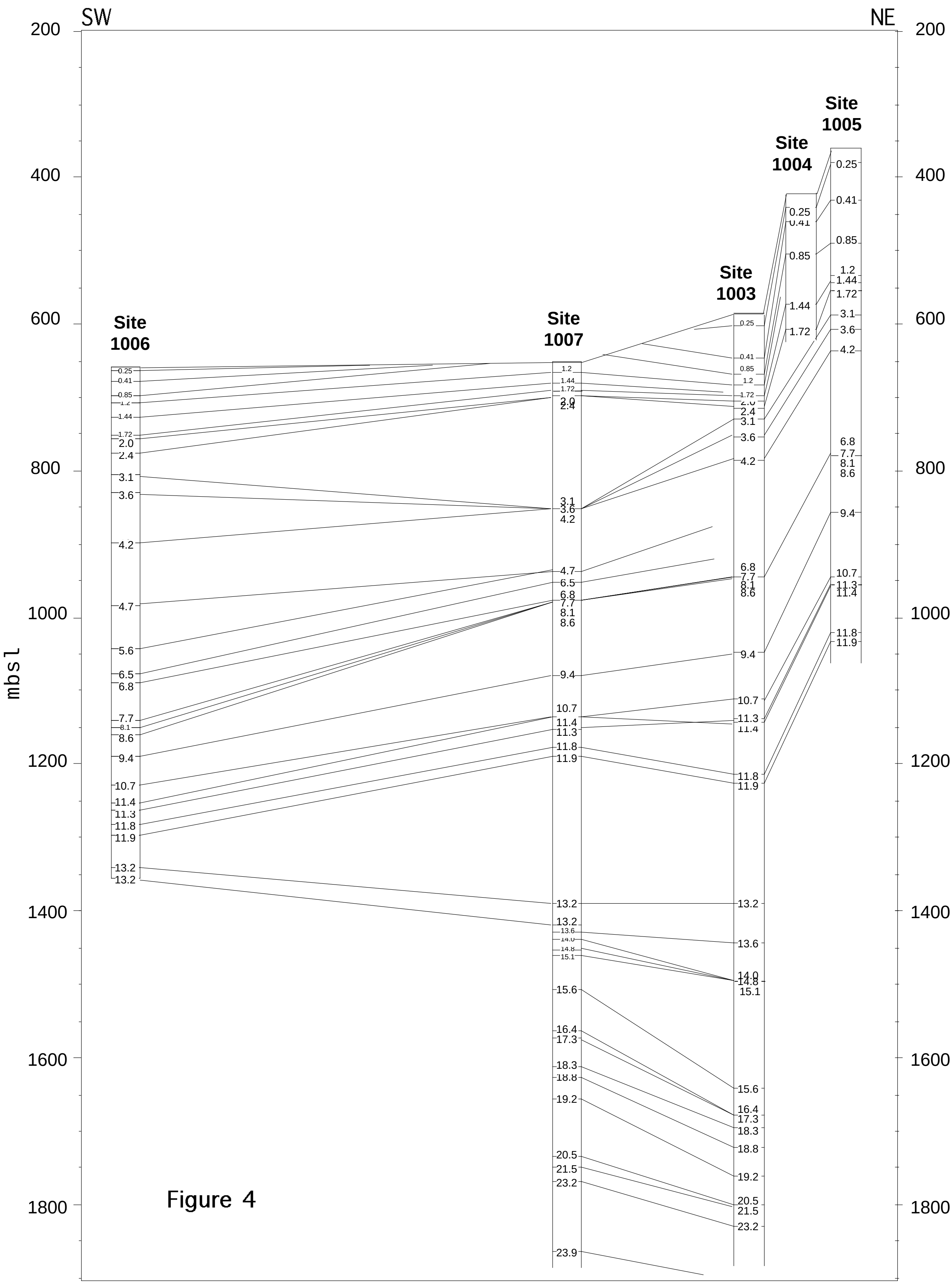
SW
NE
200
400
600
800
1000
1200
1400
1600
1800
mbsl
Site 1006
Site 1007
Site 1003
Site 1004
Site 1005

Figure 4

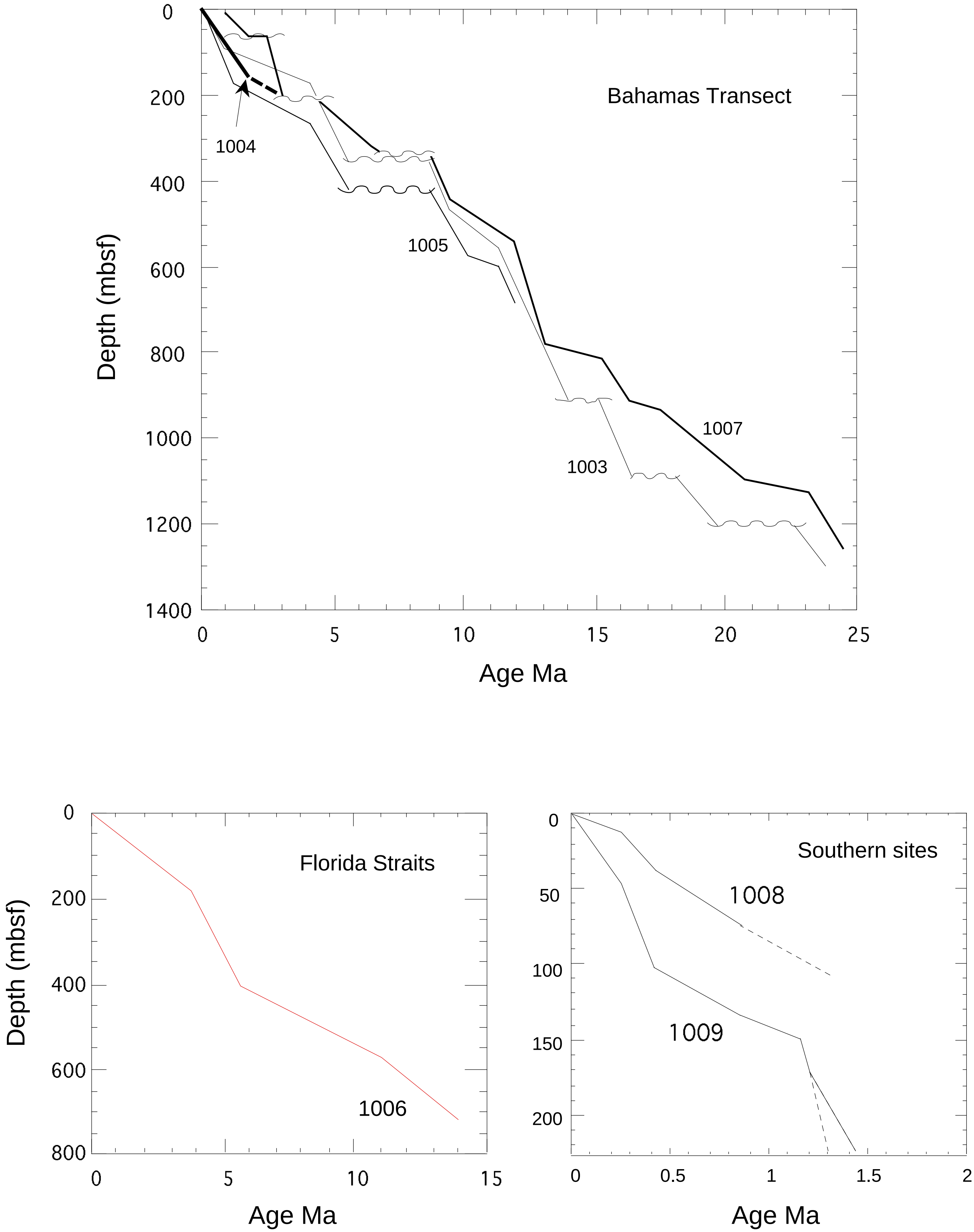

Bahamas Transect
1004
1005
1007
1003
Depth (mbsf)
Age Ma
0
200
400
600
800
1000
1200
1400
0
5
10
15
20
25
Florida Straits
1006
Southern sites
1008
1009
0.5
1
1.5
2
50
100
150

Figure 5

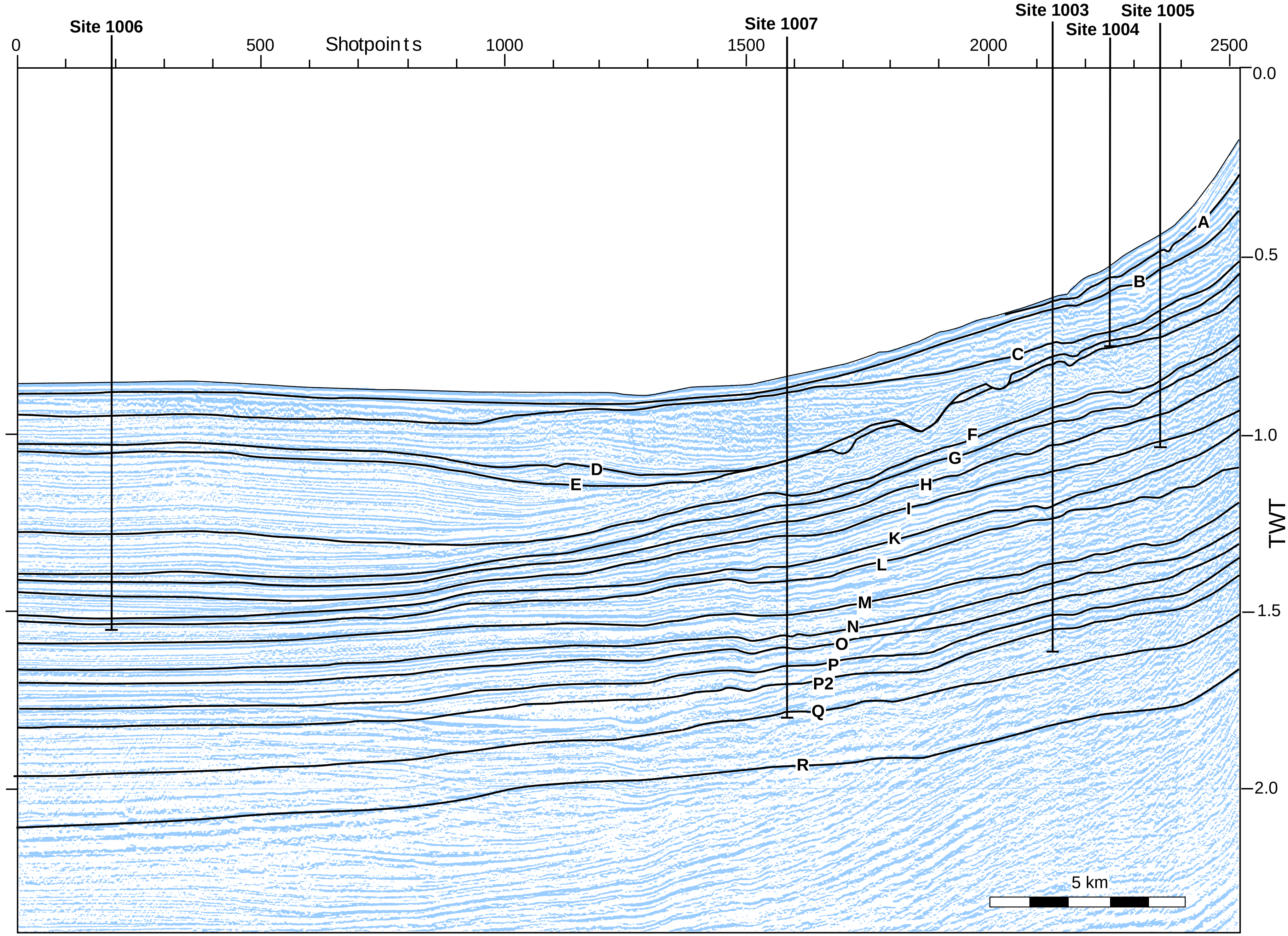
Site 1006
Site 1007
Site 1003
Site 1004
Site 1005
Shotpoints
0
500
1000
1500
2000
2500
0.0
0.5
1.0
1.5
2.0
TWT
A
B
C
D
E
F
G
H
I
K
L
M
N
O
P
P2
Q
R
5 km

Figure 6

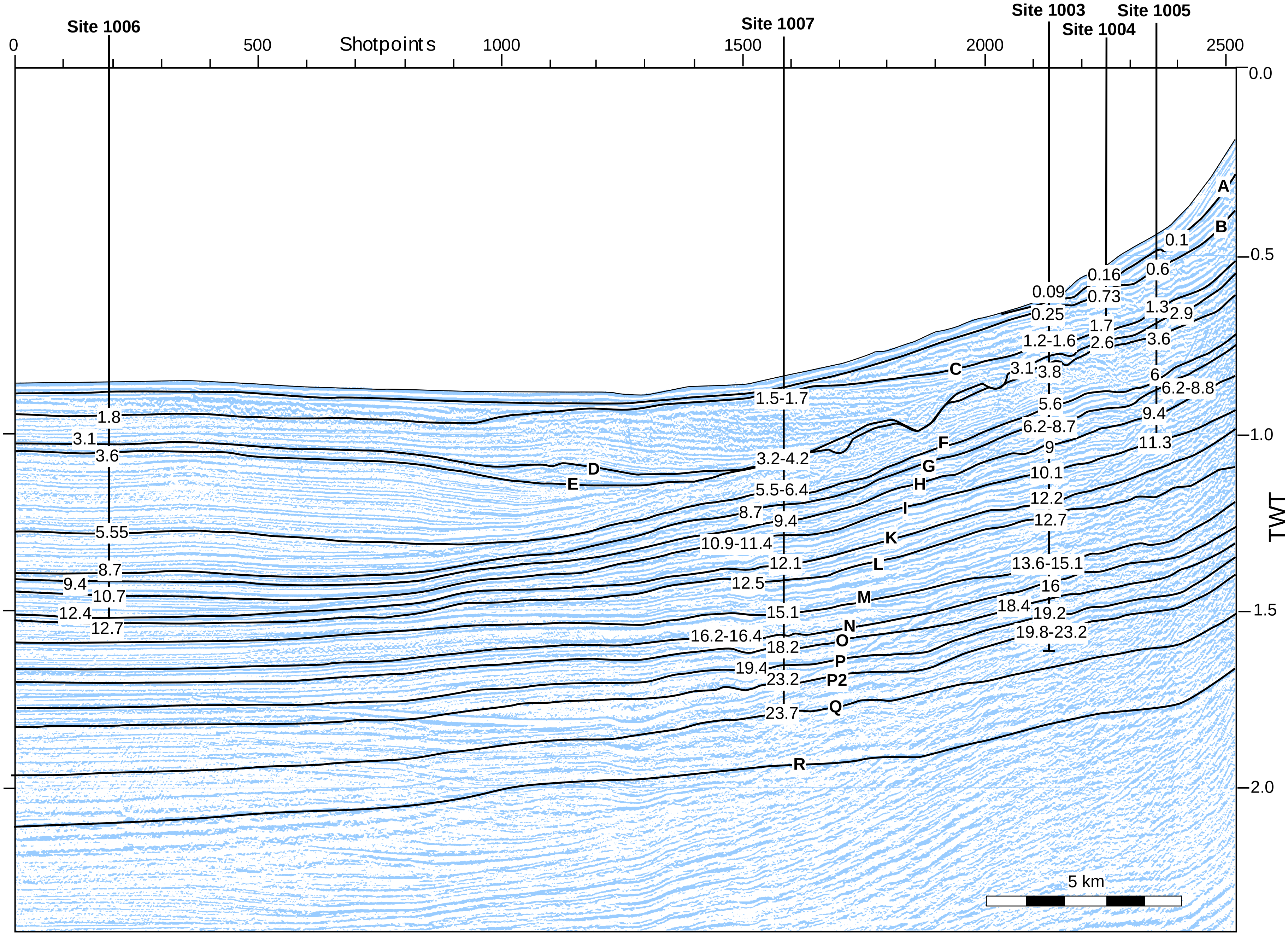

Site 1006
Site 1007
Site 1003
Site 1004
Site 1005
Shotpoints
0
500
1000
1500
2000
2500
TWT
0.0
0.5
1.0
1.5
2.0
A
B
C
D
E
F
G
H
I
K
L
M
N
O
P
P2
Q
R
5 km

Figure 7

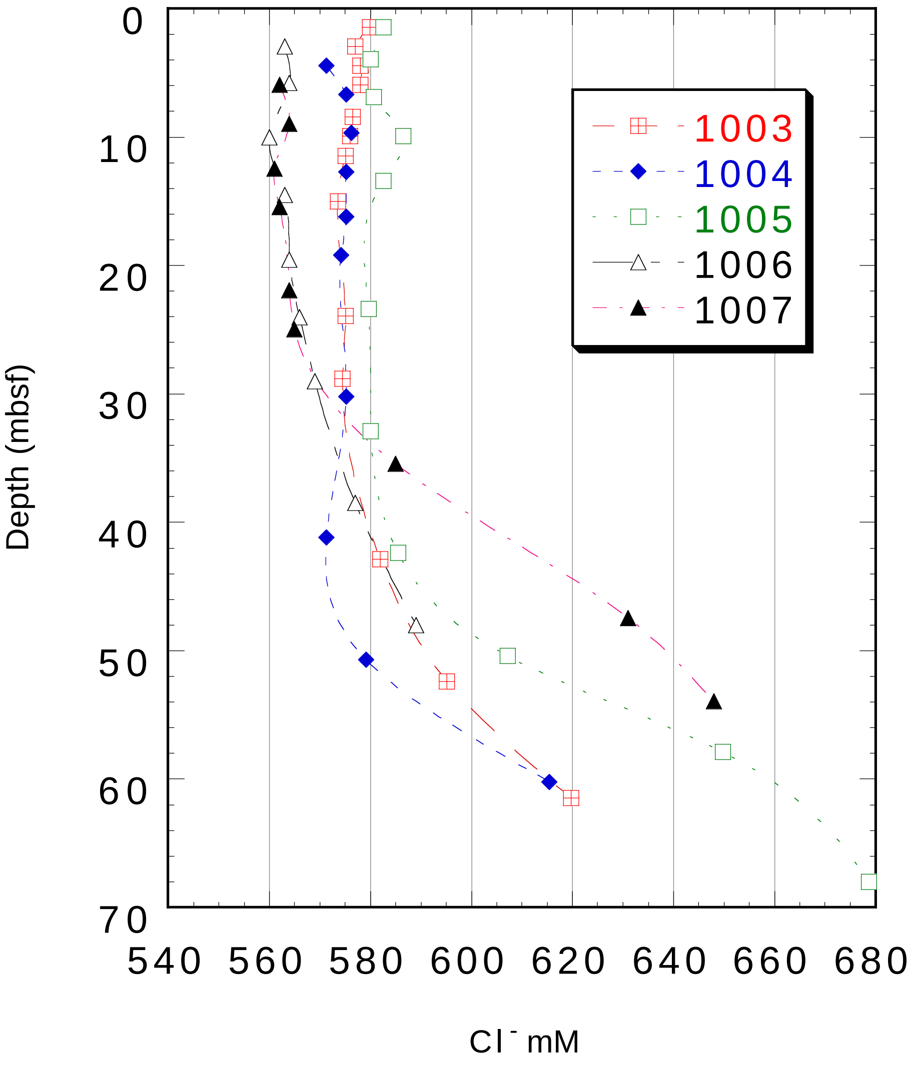

Depth (mbsf)
0
10
20
30
40
50
60
70
540
560
580
600
620
640
660
680
Cl⁻ mM
1003
1004
1005
1006
1007

Figure 8

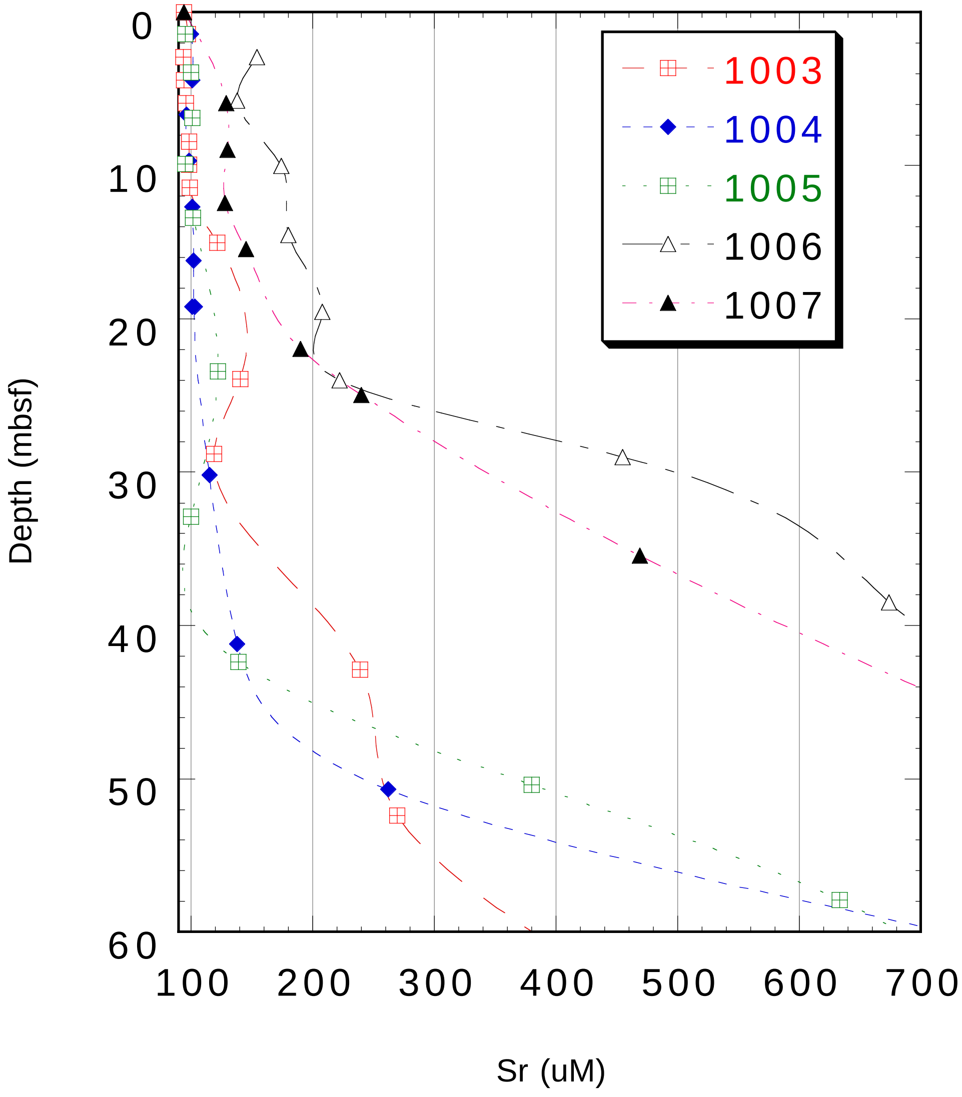

1003
1004
1005
1006
1007
0
10
20
30
40
50
60
Depth (mbsf)
100
200
300
400
500
600
700
Sr (uM)

Figure 9

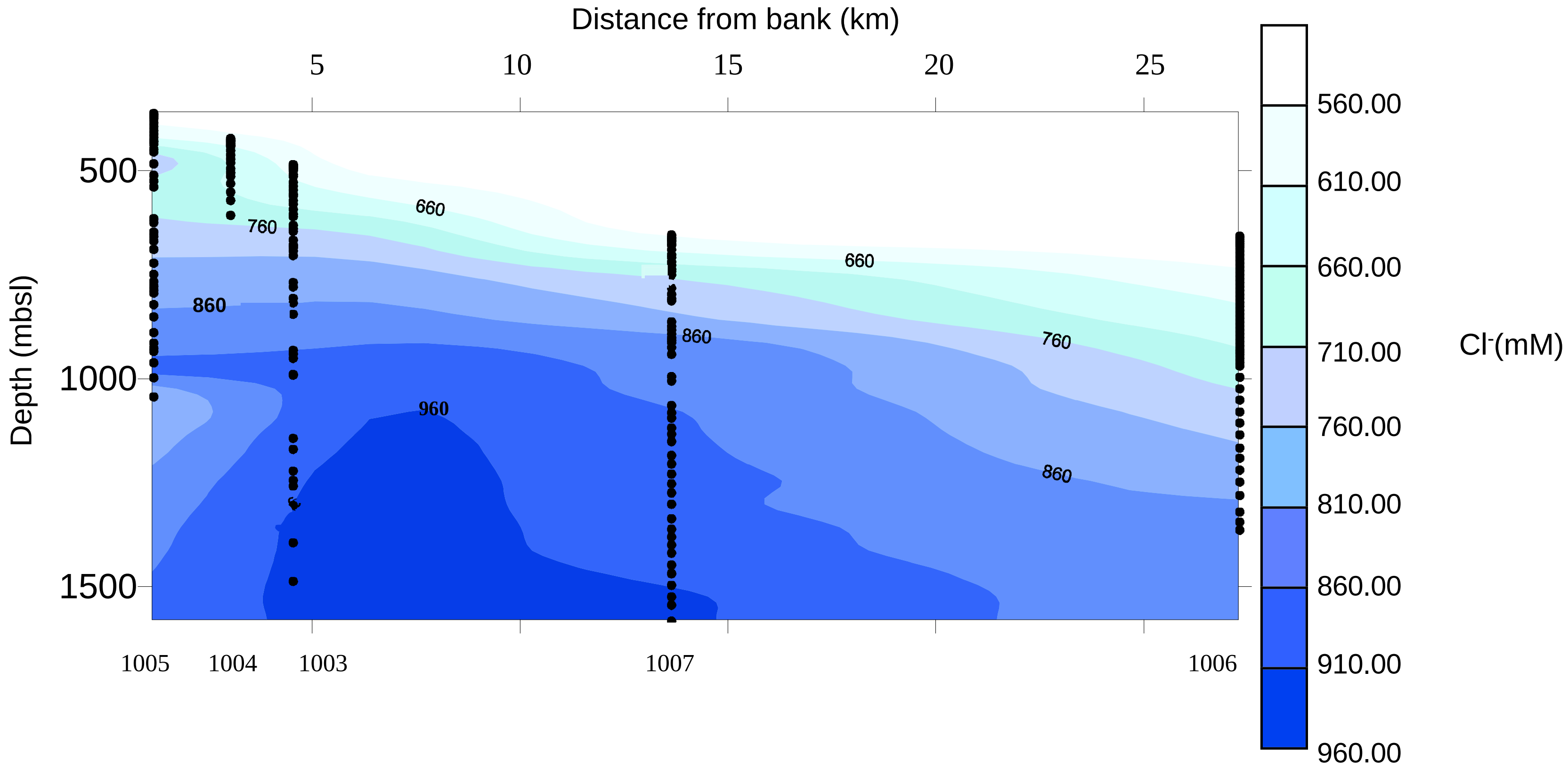
Distance from bank (km)
5
10
15
20
25
Depth (mbsl)
500
1000
1500
660
760
860
960
660
860
760
860
1005
1004
1003
1007
1006
560.00
610.00
660.00
710.00
760.00
810.00
860.00
910.00
960.00
Cl-(mM)

Figure 10

OPERATIONS REPORT

The ODP Operations and Engineering personnel aboard *JOIDES Resolution* for Leg 166 were:

Operations Superintendent:	Gene Pollard
Schlumberger Engineer:	Steve Kittredge
ODP Development Engineer:	Mark Robinson

TRANSIT FROM SAN JUAN, PUERTO RICO TO SITE 1003

The ship departed San Juan at 1709 hr on 20 February 1996. All times reported in this report are in local time (US Eastern Time Zone; UTC-5 hr). The 857-nmi sea voyage to the first way point to begin the seismic survey required approximately 68 hr at 12.5 kt average speed.

A 30-nmi seismic reflection survey was conducted over Sites 1003, 1004, 1005, 1006, and 1008 (Proposed Sites BT-2/F-2, F-3, BT-1A/F-1, BT-20, BT-3, respectively) in 4.7 hr at 6.3 kts. The ship returned to the GPS coordinates for Site 1003.

SITE 1003
(Proposed Site BT-2)

We deployed a Datasonics commandable retrievable beacon at 24°32.746'N, 79°15.642'W on 1812 hr, 23 February 1996. Unless otherwise noted, depths in the operations section within individual site reports refer to meters below rig floor (mbrf). This depth is calculated using the drill pipe measurement (DPM) from the top of the dual elevator stool (DES) on the rig floor. The distance from the dual elevator stool (DES) to sea level varies over time, depending on the ship's draft.

Hole 1003A

An advance hydraulic piston corer/extended core barrel (APC/XCB) bottom hole assembly (BHA) was attached to monel drill collars. Monel drill collars are intended to minimize remagnetization, allowing magnetic orientation of the APC cores. Hole 1003A was spudded at 2215 hr on 23 February. Core 1003A-1H was cut with the drill bit positioned at 490.0 mbrf. Core 1H recovered 6.97 m; therefore, the seafloor was defined to be 492.5 mbrf. The distance between the DES and sea level at Hole 1003A was 11.1 m, making the water depth 481.4 meters below sea level (mbsl).

Adara heat measurements were taken at Cores 3H through 9H. Core orientation using the tensor tool was performed on Cores 4H through 9H. Using the APC, we cored 77.7 m recovering 69.85 m (89.9% recovery). Recovery was reduced by common hard carbonate layers/nodules and occasional sandy carbonate layers in soft carbonate ooze. Core 9H (77.7 mbsf) was a partial stroke with a split core liner and required 60,000 lb overpull to extract the core barrel from the formation. We then switched to the XCB coring method.

XCB cores were cut from Core 10X through 21X (77.7-188.1 mbsf). WSTP temperature measurements were performed after Cores 3X, 6X, 9X, and 22H. Recovery ranged from 0 to 100% (mean = 44%). Cores 17X and 18X had carbonate nodules jammed in the shoe and Cores 20X and 21X had no recovery in a very soft formation, resulting in heavy backflow.

APC Core 22H was taken from 188.1 to 197.6 mbsf with 103% recovery. The APC barrel stuck and could not be extracted from the formation with 60,000 lb overpull. The bit nozzles became plugged with cuttings that flowed back into the pipe, stalling the rotary, and packing off the annulus. Overpull was gradually increased until circulation and rotation were restored. Although several nozzles remained plugged, XCB coring was resumed.

XCB Cores 23X to 27X were cut from 197.6 to 245.7 mbsf with 1.3% recovery. The bit nozzles remained plugged and heavy backflow was observed. Consequently, the hole was terminated and the bit cleared the rig floor at 2200 hr on 24 February.

Hole 1003B

The ship was moved 20 m to the northwest and Hole 1003B was spudded at 0105 hr, 25 February. Core 1003B-1H was taken with the drill bit positioned at 488.0 mbrf. Recovery of the mudline core defined the seafloor at 483.3 mbsl. APC cores were taken from Core 1H to 9H (0 to 79.0 mbsf) with 80.7% recovery. No oriented cores were taken. An Adara temperature tool heat-flow measurement was taken during Core 8H. APC coring was terminated at 79.0 mbsf with 60,000 lb overpull.

XCB cores were cut from Core 10X to 57X (79.0 to 541.6 mbsf) with recovery varying from 0 to 100% (mean=27%). The WSTP was deployed after Core 11X. Recovery was reduced by moderately hard layers that jammed in the shoe. Recovery was low in formation sections that alternated between lithified and unlithified. The pump rate was reduced in soft carbonates to reduce washing and was increased in harder carbonates to reduce jamming. The formation sections became noticeably harder at 34X (310.6 mbsf), 40X (368.2 mbsf), and 52X (483.9 mbsf) with increased drilling time and torque and reduced recovery. Hole 1003B was terminated and the bit cleared the rig floor at 1545 hr, 26 February.

Hole 1003C

The ship was moved 10 m northwest of Hole 1003B. Hole 1003C was spudded using the rotary core barrel (RCB) system at 2020 hr on 26 February. The water depth was assumed to be 483.3 mbsl based on adjacent Hole 1003B. The hole was drilled from 0 to 406.0 mbsf. Cores 1003C-1R to 2R were cut from 406.0 to 425.3 mbsf. After retrieving Cores 1R and 2R, the hole was drilled from 425.3-473.5 mbsf. RCB Cores 3R to 88R were then cut from 473.5 to 1300.0 mbsf. From the original approval depth of 1050 mbsf, Hole 1003C was deepened to 1300 mbsf to reach the base of the Neogene after which coring was terminated. Recovery using the RCB system ranged from 4.1 to 103.0% (mean = 44.7%). At least 21 cores were jammed from fractured core sections wedging in the shoe and liner. A strong petroleum odor was noted in Cores 30R to 41R (732.4-842.0 mbsf), with increasing amounts of heavier hydrocarbons (C_2-C_6) observed in headspace analyses. C_1/C_2 ratios decreased from 23 to 8. However, coring continued on a core-to-core basis because the concentration of gas was very low, and there were no rapid changes in gas concentration or C_1/C_{2+} ratios (C_1/C_2 ratios being already anomalously low from the top of the hole).

During the process of cleaning the hole in preparation for logging, the drill pipe became stuck. For five hours we unsuccessfully attempted to free the pipe using up to the maximum overpull allowed for shallow-water drilling (200,000 lb). The pipe was severed at 1008.5 mbsf with an explosive charge. The severed pipe was pulled to 96 mbsf and we dropped a free-fall funnel (FFF). The vibration-isolation tool was deployed with a television camera and sonar to verify positioning of the FFF and the drill string was pulled out of the hole. A RCB BHA was deployed and the hole was re-entered for logging. However, the drill pipe became stuck again while attempting to condition the hole and we were not able to penetrate deeper than 465 mbsf. We encountered similar conditions while pulling up the drill string suggesting the upper part of the hole was collapsing. Therefore, we judged it imprudent to make any further attempts to log the hole. Hole 1003C was terminated and the bit cleared the rig floor at 1457 hr, 6 March.

Hole 1003D

After evaluating hole stability and logging potential at several sites, we returned to Site 1003 on March 20 to drill a dedicated logging hole. The 14.0 nmi transit from Site 1006 to Site 1003 required 4.25 hr. After positioning the ship on the GPS coordinates (24°32.763'N, 79°15.650'W), a beacon was dropped at 0530, 20 March. A drilling BHA was assembled and run to the seafloor (482.9 mbsl). The hole was drilled to 677.0 mbsf and then conditioned with a short trip from 677.0 to 536.0 mbsf with no overpull or drag. Drilling was resumed from 677.0 to 1052.7 mbsf. A standard wiper trip was performed to 100 mbsf encountering 2.5 m of soft fill, and the bit was released with an MBR. After a circulating a sweep of sepiolite mud, the pipe was pulled to 106 mbsf for logging. Phasor dural induction tool (DIT)/Sonic, Formation MicroScanner (FMS), integrated porosity lithology tool (IPLT), induced gamma-ray spectroscopy (GST), and VSP logs were run to 1052.7 mbsf. After plugging the hole with cement and gel mud, the pipe was pulled and secured for transit at 0723 hr on 24 March. Although the beacon indicated release, it did not surface and could not be retrieved.

SITE 1004
(Proposed Site F-3)

Hole 1004A

The ship was moved 0.8 nmi to the GPS coordinates for Site 1004 at 24°33.283'N, 79°14.95'W. A beacon was dropped and coring at Hole 1004A was initiated at 2010 hr on 6 March. The water depth was 418.9 mbsl based on recovery of the mudline core. APC Cores 1004A-1H to 12H were cut from 0 to 102.8 mbsf with recovery ranging from 2.1 to 103% (mean = 87.8%). Cores were oriented for Cores 3H-7H and 9H-11H, and Adara temperature tool heat-flow measurements were taken during coring of Cores 4H through 8H, 10H, and 12H. Recovery was reduced by hard layers jamming in the throat of the bit; therefore, we switched to the XCB coring system. XCB Cores 13X to 23X were cut from 102.8 to 200 mbsf with recovery varying from 0 to 82.8% (mean = 28.1%). Coring was terminated when objectives for Site 1004 were achieved and the bit cleared the seafloor at 1815 hr on 7 March.

SITE 1005
(Proposed Site BT-1/F-1)

Hole 1005A

The ship was moved 0.9 nmi to the GPS coordinates for Site 1005, and Hole 1005A was initiated at 2000 hr, 7 March. The water depth was determined to be 350.7 mbsl based on recovery of the mudline core. APC Cores 1005A-1H to 9H were cut from 0 to 67.5 mbsf with 101.3% recovery, orienting Cores 3H-9H with the tensor tool. Adara temperature tool heat-flow measurements were deferred until Hole 1005B to determine the approximate depth of hard layers that might damage the tool. As in the previous two sites, recovery was reduced by hard layers jamming in the throat of the bit. Core liners shattered on Cores 8H and 9H, prompting a change to the XCB coring system. XCB Cores 10X to 53X were cut from 67.5 to 462.4 mbsf with 20.6% recovery. Cores 14X to 29X and 37X to 53X had only 12% recovery in soft, gassy, sediments with lithoclasts and occasional cemented layers, despite using minimal circulation rates. The pipe became stuck while cutting Core 38X at 686.2 mbsf, when the hole apparently collapsed, packing off the annulus and stalling the rotary. The formation was fractured and the drill string was eventually worked free after circulation and rotation were re-established. Subsequently, the hole was back-reamed to 172 mbsf, and then reamed to bottom. WSTP temperature probes were deployed after Cores 11X, 14X, 19X, and 22X. As a result of the unstable hole conditions, a precautionary short trip was made to 255.6 mbsf to condition the hole prior to logging.

Because of the previous difficulty logging Hole 1003C, we chose to log Hole 1005A rather than risk not obtaining any logging data, if similar unstable hole conditions were encountered in Hole 1005C. Therefore, XCB coring was terminated at 462.4 mbsf as the result of poor recovery. The bit was pulled up to the logging depth at 103.8 mbsf. A Sonic/DIT log was run to 445 mbsf, and an IPLT log was run to 434 mbsf. Finally, a VSP log was run to 409 mbsf. After running the VSP experiment in the open hole, the VSP tool would not reenter the bit because the hydraulic clamping arm would not retract; therefore, a Kinley crimper and cutter tools were dropped to clamp the line inside the BHA and then sever the logging line above the tool. The VSP tool was retrieved intact and the pipe cleared the rotary at 2030 hr on 10 March.

Hole 1005B

Coring at Hole 1005B was initiated 10 m to the south of Hole 1005A. The hole was spudded at 0011 hr on 11 March using the same APC BHA without the nonmagnetic drill collars (NMDC). Hole 1005B was drilled primarily to obtain heat-flow measurements. The water depth was determined to be 351.7 mbsl based on recovery of the mudline core. APC Cores 1005B-1H to 7H were cut from 0 to 51.0 mbsf with 81.4% recovery. Adara temperature tool heat-flow measurements were taken during coring of Cores 3H through 7H. Core 7H was a partial stroke that threw slack in the coring wireline where it entangled on the heave compensator and the line subsequently parted. After restringing the wireline, Core 7H was retrieved. XCB Core 8X was taken from 51.0 to 52.0 mbsf to penetrate a hard layer, and XCB Core 9X was cut from 52.0 to 61.7 mbsf. A WSTP temperature probe was deployed after Cores 8X and 9X. With the objectives of Hole 1005B achieved, the hole was terminated and the bit cleared the rotary table at 1305 hr on 11 March.

Hole 1005C

The ship was moved 20 m south of Hole 1005B, and Hole 1005C was initiated with a RCB BHA with a mechanical bit release (MBR) at 1750 hr on 11 March. The water depth was estimated to be 351.6 mbsl based on bit contact. A hole was drilled with a center bit to 386.6 mbsf. RCB Cores 1R to 34R were cut from 386.6 to 700.0 mbsf with 34.1% recovery.

A conditioning trip for logs was made to 85.5 mbsf and the bit was released using the MBR, the hole was filled with sepiolite mud, and the open drill string was positioned at 398.3 mbsf. The following suite of logs were run: (1) an IPLT log to 700.0 mbsf; (2) a DIT/Sonic log to 693.0 mbsf; (3) a FMS to 613 mbsf; and (4) a VSP log to 541 mbsf. The FMS and VSP logs were lighter weight tools that limited the ability to work them deeper into the hole. After plugging the hole with cement and gel mud, the pipe was pulled and secured for sea voyage at 0854 hr on 15 March.

SITE 1006
(Proposed Site BT-5)

Transit: Site 1005 to Site 1006

The transit from Site 1005 to Site 1006 covered approximately 15.6 nmi in just over 1.5 hr. We proceeded directly to GPS coordinates 24°23.989’N, 79°27.541’W and deployed a retrievable beacon at 1054 hr, 15 March.

Hole 1006A

We assembled a BHA similar to that used at the previous sites and ran the bit to the seafloor. Hole 1006A was initiated at 1355 hr on 15 March. The water depth was 657.9 mbsl based on recovery of the mudline core. Continuous APC cores were cut to 273.1 mbsf with 97.4% recovery. Cores 1006A-3H-29H were oriented. Adara temperature tool heat-flow measurements were taken from Core 3H-11H, and every third APC core thereafter. Core 29H was required 80,000 lb, therefore, APC coring was terminated. XCB Cores 30X to 77X were cut from 273.1 to 717.3 mbsf with 82.5% recovery. WSTP temperature probes were deployed after Cores 32X, 35X, 38X, and 43X. Core jamming in the core catcher or core liner was observed in 14 of the last 19 cores. Coring operations were terminated at 717.3 mbsf when the objectives for this hole were achieved. A standard conditioning trip was made and the drill string was positioned at 104 mbsf for logging. The following logging runs were performed to total depth (717 mbsf) without incident: DIT/Sonic, IPLT/GR, FMS, and a VSP experiment. The bit cleared the seafloor at 0940 hr on 19 March.

Hole 1006B

The ship was moved 20 m west, and Hole 1006B was spudded at 1045 hr on 19 March. The water depth was 657.5 mbsl based on recovery of the mudline core. APC Cores 1006B-1H to

19H were cut from 0 to 176.5 mbsf with 103.2% recovery. Cores were oriented from Core 3H. The bit cleared the seafloor at 1955 hr on 19 March.

Hole 1006C

Hole 1006C was spudded to acquire a single, oriented mudline core in an attempt to obtain sediments recording the Blake paleomagnetic event that appeared to be present in the top few meters of the unoriented, first core of each of the previous two holes. The ship was moved 20 m west, and Hole 1006C was initiated at 2045 hr on 19 March. The water depth was 658.4 mbsl based on recovery of the core. APC Core 1006C-1H was cut from 0 to 6.6 mbsf with 99% recovery; however, the core liner was badly splintered. Coral debris was found in the shoe and is probably responsible for what appears to be a liner impact failure. Consequently, the hole was terminated.

Hole 1006D

The ship was not moved, and another single, oriented mudline core was attempted. Hole 1006D (Site BT-5) was spudded at 2200 hr on 19 March. The water depth was 668.9 mbsl based on recovery of the core. APC Core 1006C-1H was cut from 0 to 7.6 mbsf with 100% recovery. The drill pipe was pulled and secured at 0113 hr on 20 March.

SITE 1007
(Proposed Site BT-3)

Transit: Site 1003 to Site 1007

The 4.2 nmi transit to Site 1007 was made in dynamic positioning mode while tripping pipe and handling the BHAs. A retrievable beacon was dropped at 0755 hr on the GPS coordinates for Site 1007 (24°30.26'N, 79°19.34'W).

Hole 1007A

An APC/XCB BHA, similar to that used at previous sites, was assembled and run to the seafloor. Hole 1007A was spudded at 1110 hr on 24 March. On Core 1007A-1H, the flapper core catcher remained open and some core fell out on the rig floor. The core had a good mudline and was archived as 6.65 m recovery; however, another mudline core was taken as a precaution. The water depth was 650.3 mbsl based on recovery of the mudline core.

Hole 1007B

The ship was not moved and Hole 1007B was initiated at 1135 hr on 24 March. Core 1H recovered 9.90 m of core and appeared to have a good mudline. The water depth was 647.4 mbsl based on recovery. APC Cores 1007B-1H to 10H were taken from 0 to 38.0 and 40.0 to 91.7 mbsf with 97.1% recovery. The APC core attempt after Core 4H was rejected at 38.0 mbsf. A 1-m-thick hard layer (38-39 mbsf) was penetrated by drilling 2 m (38.0-40.0 mbsf), and APC coring was resumed. Adara temperature tool heat-flow measurements were taken during coring of Cores 4H-10H. APC coring was terminated due to core disturbance from six successive partial strokes and overpull (Cores 5H-10H). XCB cores 11X to 41X (91.7-377.7 mbsf) were cut with 38.9% recovery. WSTP temperature probes were deployed after Cores 14X, 17X, 22X, and 27X. XCB coring was terminated when core recovery became unsatisfactory (13%) in the last nine cores. The hole was filled with 130 bbl of mud and the bit cleared the rotary table at 2245 on 25 March.

Hole 1007C

The ship was moved 20 m to the southwest, and a RCB BHA similar to that used at the previous sites was run to the seafloor, which was tagged with the bit at 647.3 mbsl. Hole 1007C was initiated at 0340 hr on 25 March and drilled from 0 to 302.0 mbsf. RCB cores were cut from 302.0 to 1235.4 mbsf with 53.9% recovery. Three wiper trips were required to condition the hole while RCB coring. A short trip was made from 504 to 357 mbsf without incident. Below 750 mbsf, overpull and drag increased from 10,000 to 20,000 lb, requiring a second short trip. A third wiper trip was made at 821 mbsf, with 80,000 lb overpull noted at 277 mbsf. The drill string had to be back-reamed out of the hole through numerous tight spots to 78.4 mbsf. No ledges or fill were noted in running pipe back to the bottom of the hole and RCB coring continued from 821.4 to 1235.4 mbsf (total depth). Coring was terminated after penetrating the base of the Neogene. A gel mud sweep was circulated, and a conditioning trip for logs was made to 76.2 mbsf, with overpull at 171, 159, and 102 mbsf (50,000 lb). The bit had to be reamed back to bottom from 1141.0 to 1235.4 mbsf. The bit was released and the pipe was positioned at 111.5 mbsf. A quad-combo log was run to 1158 mbsf. The FMS log had to be canceled because of large hole diameter; therefore, a VSP log was run to 1093 mbsf. The VSP tool could not be pulled back into the bit with 4000 lb overpull. As at Site 1005, the Kinley crimper and cutter were used to cut the logging line, and the VSP tool was retrieved. The ship was under way to Site 1008 at 2018 hr on 3 April.

SITES 1008/1009
(Proposed Sites F-4 and F-6)

Transit from Site 1007 to 1008

The 55 nmi sea voyage to Site 1008 was made in 4.75 hr. A stand of drill collars was inspected during the transit, and an APC BHA was assembled. A Datasonics 354M beacon was dropped at 0105 hr on 4 April.

Hole 1008A

Hole 1008A was spudded at 0339 hr on 4 April. The water depth was 437.1 mbsl based on recovery of the mudline core. APC Cores 1008A-1H to 10H were taken from 0 to 78.7 mbsf with 100.7% recovery. Adara temperature tool heat-flow measurements were taken during coring of Cores 3H through 8H. The same cores were also oriented. A very hard layer was drilled from 34.1 to 35.1 mbsf. Core 9H required 80,000 lb overpull after washing for three minutes. Core 10H was rejected in a carbonate gravel; therefore, XCB coring was initiated. XCB Cores 11X-16X were cut from 78.7 to 134.5 mbsf with 12.3% recovery. The WSTP was deployed after Core 14X. XCB recovery was very poor in soft sediments with sporadic hard layers. Coring was terminated when the available operating time for this site was depleted. The bit cleared the seafloor at 1520 hr on 4 April.

Transit for Site 1008 to Site 1009

The 1.8-nmi transit to Site 1009 was made in dynamic positioning mode with the BHA suspended at 250 mbrf. A Datasonics 354M beacon was dropped at 1658 hr on 4 April. The drill site was moved about 73 m east of the original GPS site coordinates to obtain a thicker Holocene section.

Hole 1009A

Hole 1009A was initiated at 1825 hr on 4 April. The water depth was 307.9 mbsl based on recovery of the mudline core. APC Cores 1009A-1H to 16H were taken from 0 to 113.8 mbsf with 99.3% recovery. Adara temperature tool heat-flow measurements were taken during Cores 3H through 7H. The same cores were also oriented. A very hard layer was drilled from 22.0 to 23.5 mbsf. Core 7H was a full stroke that would not pull free with 50,000 lb overpull and was drilled over 6 m. The APC was advanced as far as possible; however, 6 cores had imploded tops or shattered liners and 7 of 16 cores were partial strokes because of the occurrence of sporadic hard layers. Consequently, we switched to the XCB coring system after Core 16H. XCB Cores 1008A-17X to 28X were cut from 113.8 to 226.1 mbsf with 69.6%

recovery. Four of 12 XCB cores were jammed in the liner or core catcher. The WSTP was deployed after Cores 11X, 14X, 18X, 21X, and 24X. Coring was terminated when the available time ran out. The BHA was secured for sea voyage at 1600 hr on 5 April.

Sea Voyage from Site 1009 to Panama

The sea voyage from Site 1009 to Panama covered 1100 nmi in about 95.6 hr. Leg 166 ended with the first line ashore in Panama at 1600 hr, 10 April.

Ocean Drilling Program
Operations Resume
Leg 166

Total Days (17 February to 10 April 1996)		52.72
Total Days in Port (Repairs)		4.63
Total Days Underway		6.80
Total Days on Site		41.29
	days	
Tripping Time	3.77	
Coring	24.39	
Reentry Time	0.00	
W.O.W.	0.00	
Stuck pipe/Hole trouble	0.000	
Drilling	4.16	
Mechanical Repair Time (Contractor)	0.00	
Logging/Downhole Science	6.83	
Other	0.20	

Total Distance Travelled (nautical miles)	2045.0
Average Speed Transit (knots)	11.9
Number of Sites	7
Number of Holes	17
Number of Cores Attempted	572
Total Interval Cored (m)	5254.9
Total Core Recovery (m)	2933.8
% Core Recovery	55.8
Total Interval Drilled (m)	2197.5
Total Penetration	7452.4
Maximum Penetration (m)	1300.0
Minimum Penetration (m)	6.6
Maximum Water Depth (m from drilling datum)	669.9
Minimum Water Depth (m from drilling datum)	319.7

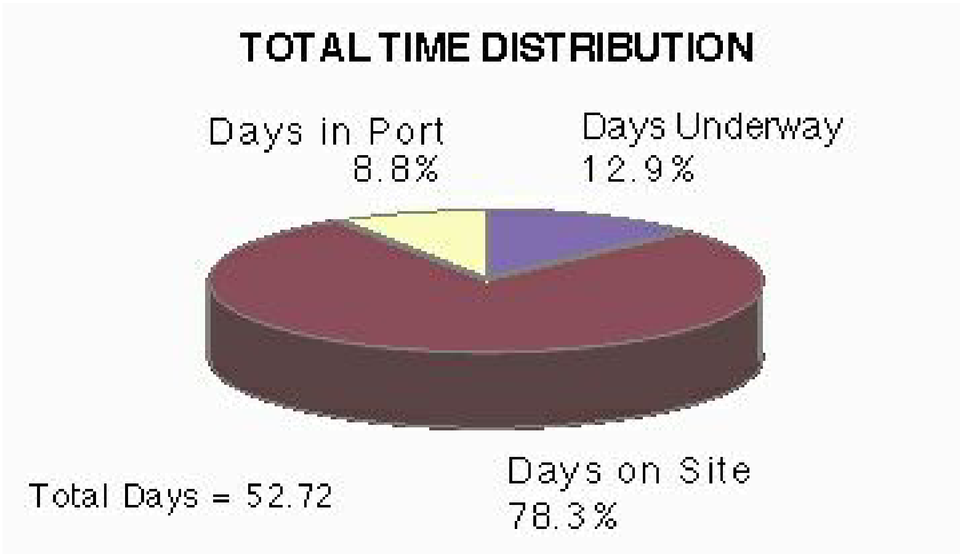
TOTAL TIME DISTRIBUTION
Days in Port
8.8%
Days Underway
12.9%
Days on Site
78.3%
Total Days = 52.72

OCEAN DRILLING PROGRAM
SITE SUMMARY
LEG 166

HOLE	LATITUDE	LONGITUDE	SEA FLOOR DEPTH (mbrf)	NUMBER OF CORES	INTERVAL CORED (meters)	CORE RECOVERED (meters)	PERCENT RECOVERED (percent)	DRILLED (meters)	TOTAL PENETRATION (meters)	TIME ON HOLE (hours)	TIME ON HOLE (days)
1003A	24°32.746'N	79°15.642'W	492.5	27	245.7	129.12	52.6%	0.0	245.7	27.75	1.16
1003B	24°32.759'N	79°15.648'W	494.5	57	541.6	187.44	34.6%	0.0	541.6	41.75	1.74
1003C	24°32.763'N	79°15.650'W	494.5	88	845.8	378.06	44.7%	454.2	1300.0	215.25	8.97
1003D	24°32.763'N	79°15.650'W	494.5	0	0.0	0.00	0.0%	1052.7	1052.7	98.00	4.08
		BT-2 / F-2 SITE TOTALS:		**172**	**1633.1**	**694.62**	**42.5%**	**1506.9**	**3140.0**	**382.8**	**15.95**
1004A	24°33.283'N	79°14.950'W	430.2	23	200.0	117.49	58.7%	0.0	200.0	27.50	1.15
		F-3 SITE TOTALS:		**23**	**200.0**	**117.49**	**58.7%**	**0.0**	**200.0**	**27.50**	**1.15**
1005A	24°33.772'N	79°14.141'W	362.0	53	462.4	149.59	32.4%	0.0	462.4	72.50	3.02
1005B	24°33.766'N	79°14.142'W	363.0	9	61.7	49.45	80.1%	0.0	61.7	16.50	0.69
1005C	24°33.755'N	79°14.141'W	363.0	34	313.4	107.00	34.1%	386.6	700.0	92.0	3.83
		BT-1A / F-1 SITE TOTALS:		**96**	**837.5**	**306.04**	**36.5%**	**386.6**	**1224.1**	**181.00**	**7.54**
1006A	24°23.989'N	79°27.541'W	669.4	77	717.3	647.11	90.2%	0.0	717.3	94.75	3.95
1006B	24°23.991'N	79°27.553'W	669.0	19	176.5	182.40	103.3%	0.0	176.5	10.25	0.43
1006C	24°23.991'N	79°27.559'W	669.9	1	6.6	6.55	99.2%	0.0	6.6	1.25	0.05
1006D	24°23.991'N	79°27.559'W	668.9	1	7.6	7.60	100.0%	0.0	7.6	4.00	0.17
		BT-5 SITE TOTALS:		**98**	**908.0**	**843.66**	**92.9%**	**0.0**	**908.0**	**110.25**	**4.59**
1007A	24°30.261'N	79°19.340'W	661.9	1	6.6	6.65	100.8%	0.0	6.6	3.50	0.15
1007B	24°30.261'N	79°19.340'W	659.0	41	375.7	198.42	52.8%	2.0	377.7	35.25	1.47
1007C	24°30.254'N	79°19.348'W	659.0	97	933.4	503.27	53.9%	302.0	1235.4	213.50	8.90
		BT-3 SITE TOTALS:		**139**	**1315.7**	**708.34**	**53.8%**	**304.0**	**1619.7**	**252.25**	**10.51**
1008A	23°36.640'N	79°05.010'W	448.9	16	134.5	86.12	64.0%	0.0	134.5	14.25	0.59
		F-6 SITE TOTALS:		**16**	**134.5**	**86.12**	**64.0%**	**0.0**	**134.5**	**14.25**	**0.59**
1009A	23°36.840'N	79°03.000'W	319.7	28	226.1	177.52	78.5%	0.0	226.1	23.00	0.96
		F-4A SITE TOTALS:		**28**	**226.1**	**177.52**	**78.5%**	**0.0**	**226.1**	**23.00**	**0.96**
		LEG 166 TOTALS:		**572**	**5254.9**	**2933.79**	**55.8%**	**2197.5**	**7452.4**	**991.0**	**41.29**

TECHNICAL REPORT

The ODP Technical and Logistics personnel aboard *JOIDES Resolution* for Leg 166 were

Miriam Andres	Marine Lab Specialist (Temporary)
Tim Bronk	Marine Lab Specialist (Chemistry)
Brad Cook	Marine Lab Specialist (Photographer)
Sandy Dillard	Marine Lab Specialist (Storekeeper)
Cesar Flores	Marine Computer Specialist (System Manager)
Margaret Hastedt	Assistant Lab Officer (Paleomagnetics)
Kuro Kuroki	Assistant Lab Officer
Monty Lawyer	Marine Lab Specialist (Underway Geophysics)
Jaque Ledbetter	Marine Lab Specialist (X-Ray)
Greg Lovelace	Marine Lab Specialist (Physical Properties)
Erinn McCarty	Marine Lab Specialist (Curator)
Bill Mills	Laboratory Officer
Chris Nugent	Marine Lab Specialist (Downhole Tools)
Anne Pimmel	Marine Lab Specialist (Chemistry)
Jo Ribbens	Marine Lab Specialist (Yeoman)
Bill Stevens	Marine Electronics Specialist
Mark Watson	Marine Electronics Specialist
Barry Weber	Marine Computer Specialist (System Manager)

GENERAL LEG INFORMATION

The *JOIDES Resolution* docked in San Juan, Puerto Rico, on 17 February 1996, ending Leg 165. The following morning the Leg 166 crew arrived and began crossovers and other logistic activities.

On the 20th of February at 1700 hr, we cast off lines and were under way to our first site with a crew of 110 (48 scientists and technicians). Our transit was uneventful and the time was effectively used for classes, completing unfinished port call activities, and preparing the labs for core analysis. In the afternoon of 23 February, an extensive site survey was completed for Sites 1003, 1004, 1005, and 1007. That same evening Hole 1003A was spudded.

During the leg we received two helicopter visits. The first visit arrived on 26 February with a film crew from New Dominion. The filming was organized by ODP's Public Relations Officer Aaron Woods. In addition, Eric Shultz, of the Borehole Research Group, arrived on the helicopter to continue repairs to the logging heave compensator. The second helicopter arrived on the 21st of March with the Public Relations Officer from Rosentiel School for Marine and Atmospheric Science (RSMAS), University of Miami and a local news crew.

Drilling operations were completed on the 5 April. After a 5-day transit, the *JOIDES Resolution* crossed the Panama Canal and docked in Balboa, Panama on the 10 April 1996, ending the scientific portion of Leg 166.

On 11 April the science party departed, and the Leg 166 technicians began logistic activities including off-loading core and loading Leg 167 supplies. Twenty-two new crew members boarded to work on various projects during the transit to Acapulco.

On the 13 April at 1715 hr, we cast off lines and were under way to Acapulco. Leg 166T ended on the 19th of April at 0800 when the ship arrived in Acapulco for a total of 60 days at sea.

LAB ACTIVITIES OVERVIEW

Although over five kilometers of sediment were cored, recovery (55.3%) kept core lab activities at a moderate pace. High-resolution water sampling, XRD analysis, and temperature measurements kept the chemistry, x-ray, and downhole labs busy.

High concentrations of H_2S (40-2700+ ppm) were encountered at almost all sites. Core lab H_2S precautions were instituted per ODP Technical Note 10. Breathing apparatus were worn as necessary while processing cores. Most cores were degassed to the outside (Sites 1004 and 1005) by using two portable exhaust fans ducted through the passive air vent in the splitting room.

CHEMISTRY LAB

Interstitial water shipboard analysis on Leg 166 included refractometric analysis for salinity; titrations for pmH, alkalinity, chloride, and fluoride; ion chromatography for sulfate, potassium, sodium, calcium, and magnesium; and colorimetric analyses for silica, phosphate, and ammonium. Atomic absorption spectrophotometry was used to quantify concentrations of Li, Sr, and Fe in pore waters. Solid core samples were analyzed for inorganic and total carbon analysis (using the coulometer and the CNS). Based on their organic carbon content, some samples were selected and analyzed with the Rock Eval. The system was used to determine S_1, S_2, S_3, S_4, and TOC. Gas chromatograph (GC) 3 and the natural gas analyzer (NGA) were used to provide real-time monitoring of the volatile hydrocarbons. GC2 was used to conduct analyses of high-molecular-weight hydrocarbons and long-chain alkenones.

COMPUTERS

This leg was marked by development of the JANUS project and the amount of self-training. Along the way we created a standard JANUS installation for the PCs and Macs and added ten more Pentiums to the ship environment. One of these Pentiums was set up as a Netware 4.1 file server and installed in the equipment room. This allowed us to decommission the Novel server “novserv1.” During the leg, we configured the accounts on both Hudson and Byrd for the JANUS project. This was done so the environment would be similar to the Sun network. To accomplish this, we edited the login scripts, moved the user directory to /home, and set up the uid’s.

CORE LAB

All the parts for the Super Saw and the Felker Saws were organized and inventoried. The bearings were changed at the beginning of the leg. The new rods and bearings brought to the ship to be installed could not be adapted to the present structure. The Minolta spectrophotometer was mounted on a track for instrument support during measurements. Future improvements will provide automatic sample position. New catwalk boxes are in the process of being designed and built, as are new liner cutters.

CURATION

Most of the deep holes drilled during this leg recovered consolidated sediments. Recovery ranged from long, continuous sections of unbroken core to small, round rollers. No shipboard PMAG samples were taken. Instead, discrete PMAG samples were taken for one of the scientists at a sampling frequency of one to two samples per section. Some of these samples were used for shipboard susceptibility measurements. All PMAG cubes will go back to Don McNeill's lab for further analyses.

DOWNHOLE MEASUREMENTS LAB

Downhole measurements conducted 87 temperature runs, setting a new record for the lab. The Adara temperature tool was run 57 times. The 30-inch WSTP tool, for temperature measurement only, was deployed 30 times. A physical inventory count was performed midway through the leg.

Because of the increase to four digit site numbers, the DCDL program has been changed. The DCDL program makes the file name out of the information entered, and because a PC won't take any file name over eight digits, listing the full site number with temperature range caused problems. To make room for the longer site numbers, the temperature range was dropped from the file name.

PALEOMAGNETICS LAB

The lab ran a total of 300 cores at various demag levels for a grand total of 1476 runs. Many discrete samples were taken for post-cruise research, and approximately 30 were measured on the spinner (mostly IRM-saturation tests). This was a difficult leg for the cryogenic magnetometer. The intensities of the carbonates were low to non-existent (generally well below 1 mA/m on the pass-through data), and most pass-through measurements were deemed of dubious value to magnetostratigraphy. Unfortunately, the new spinners couldn't measure the carbonates either. Both scientists were resigned to running the core samples when they returned to their own labs. The tensor tools oriented a total of 78 cores from 8 holes at five sites. We finally got a chance on this leg to attempt to orient the first APC core. It worked fine, although there is some pipe movement in the azimuth and inclination data, as well as somewhat higher standard deviations on the MTF results.

PALEONTOLOGY/MICROSCOPE LAB

The Leg 166 shipboard scientific party included four paleontologists; three foraminifer specialists and one nannofossil specialist, and they analyzed over 600 samples. The scientists indicated that the lab facilities and supplies were satisfactory overall. One scientist who had sailed some years previously said that the lab was "much improved" and that he was "very happy" with everything. There were no problems with any of the equipment.

In the Paleo lab, the Axiophot, both SV-11's and an SV-8 were used. In the Core lab both photoscopes were used, as were two SV-8's. No photomicrographs were taken, and everything ran smoothly during the entire cruise.

PHOTO LAB

Work was routine with a few equipment problems. The developer replenishment solenoid was replaced, and a new temperature control monitor was installed on the E6 processor. The silk-screen procedure was eliminated this cruise. A new system based on a thermal wax/dye-sublimation printer was installed. The new system prints out a copy of the winning logo onto an iron-on transfer sheet. This new method will save the photographer a great many headaches, not to mention time. During the transit the new Digital Imaging System was installed for use on Leg 167.

PHYSICAL PROPERTIES LAB

In the Physical properties lab we measured 1630 sections of core on the MST, 350 Thermal Conductivity measurements, 6412 discrete velocity measurements, 700 sheer strength measurements, and 1444 moisture/density determinations. All lab equipment performed well with few problems.

During the transit we test-fitted the new MST track hardware, took final measurements and reinstalled the old track. The final installation of the new MST track is now scheduled for Leg 169. Also, the new Moisture and Density software was tested during the transit.

UNDERWAY and FANTAIL

A seismic survey over Sites 1003, 1004, 1005, and 1007 was performed using the 80-in^3 air gun. Five VSP experiments were performed on this leg using the 120-in^3 air gun. No problems occurred during any of the experiments.

All the gun parts have been inventoried and the drawers organized. The water line to the fantail was replaced, and we now have good water pressure at this locality.

X-RAY LAB

During Leg 166, 1100 mineral samples of lithified and unlithified carbonate sediments were submitted for bulk analysis by x-ray diffraction. Thirty-seven lithified and unlithified carbonate sediment samples were analyzed with the XRF for percentages of five major element oxides (CaO, Fe_2O_3, MnO, P_2O_5, and TiO_2).

TRANSIT ACTIVITIES (166T) OVERVIEW

Five additional Tracor employees as well as four members of the JANUS Steering Committee joined the ship in Panama to continue work on the JANUS database. Daily meetings were held with Marine Specialists to discuss user group issues and answer Tracor questions.

TRANSIT PROJECT SUMMARY

- Completed a magnetic survey of coring equipment. Data from these measurements will be used to better understand the cause of magnetic over-printing of sediment during the coring process.
- Trained technicians in water-gun maintenance and thin-section preparation.
- Inventoried and organized library books and office files.
- Completed physical counts of the major storage areas.
- Installed a new version of HP ChemStation.

- Continued training of new photographer and chemist.

- Installed DCS heave compensator cabling in derrick.

- Completed shipboard GFE inventory.

- Set up the Oregon State’s color-reflectance track and the ODP core-video system for Leg 167.

- Installed and tested the new Moisture and Density software and hardware. Further revisions to the software will be necessary before shipboard implementation can proceed.

- Tested new GRAPE calibration procedures.

PROBLEMS ENCOUNTERED SUMMARY

- The slow learning curve with WinFrog continues. This leg we found that having a space in a directory name would cause WinFrog to crash anytime the waypoint data was accessed during a survey.

- Green chemical stains were found on core boxes during the San Juan port call. A leak in the photo lab plumbing was suspected but no telltale drips could be found. Towards the end of the leg the stains reappeared and the leak located. Ships engineers patched a section of the drain with rubber hose but suspect further damage and advise that all copper lines be removed and replaced with pvc in the near future.

- The XRF spectrometer chamber lid and motor where damaged early in the leg. Parts from several "used-but-good" spares were used to build a new motor and lid.

- The new rods and bearings that were brought out to be installed on the super saw could not be adapted to the present structure. The support structure is too warped for the tolerances allowed by the new type of bearings. Plans for a new support base will be developed on shore.

Leg 166 Laboratory Statistics

General	
Sites:	7
Holes:	16
Meters Drilled:	2149.3 m
Meters Cored:	5303.1 m
Meters Recovered:	2933.8 m
Number of samples:	
General Samples:	27,553
Chemistry Samples:	1,866
Lab Analysis:	
Magnetics Lab:	
Cryomagnetometer:	1476 sections
Discrete Measurements:	30
Oriented cores	78
Physical Properties:	
MST:	630 sections
Discrete Velocity:	6412
Strength:	700
Thermal Conductivity:	350
Moisture/Density:	1443
Chemistry:	
Rock Eval:	62
Water Chemistry:	260
Head Space:	470
Inorganic Carbonate:	763
Carbon Nitrogen Sulfur:	350
X-ray:	
XRF:	37
XRD:	1100
Downhole	
Adara:	57
WSTP (temp. only):	30
Thin Sections:	52
Underway Geophysics:	
Total Transit	3473 nmi
Bathymetry:	887 nmi
Magnetics:	887 nmi
Seismic	30 nmi
VSP:	5 sites